ADDIS ABABA UNIVERSITY

ADDIS ABABA INSTITUTE OF TECHNOLOGY (AAIT)

SCHOOL OF GRADUATE STUDIES

Thermal Analysis for Electric vehicle Battery Tray with Modified Material using Numerical method:

A thesis submitted to the School of Graduate Studies of Addis Ababa University in partial fulfillment of the requirement of the Degree of Master of Science in Mechanical Engineering (Mechanical Design).

By: Nigist Fentaye

Advisor: Araya Abera (PhD)

Feb, 2025 G.C

Addis Ababa, Ethiopia

Addis Ababa University

Addis Ababa Institute of Technology

School of Mechanical and Industrial Engineering

Thesis Approved by;

Submitted by:

Nigist Fentaye

Student's name **Signature** **Date**

Araya Abera (Ph.D.) _____ _____

Advisor **Signature** **Date**

Hiredin I. (Ph.D.) _____ _____

Internal Examiner **Signature** **Date**

Yilma T. (Ph.D.) _____ _____

External Examiner **Signature** **Date**

Araya Abera (Ph.D.) _____ _____

Dean, School of Mechanical and

Industrial Engineering **Signature** **Date**

Sosina Mengistu (Ph.D.) _____ _____

Associate Director of

Postgraduate program **Signature** **Date**

ACKNOWLEDGEMENT

First and foremost, I would like to express my gratitude to almighty God for his blessings. I would like to extend my heartfelt thanks to Araya Abera (phd), since he helped me to grow and exploit my potential, for his consistent consultancy, suggestion and concrete advices.

I would like to sincerely thank Eng. Mohammod for providing important data for this research. He also kindly allowed me access to the green tech company's facilities, which enabled me to measure and observe a number of components that were necessary to carry out this study. Additionally, I would like to thank my classmates for their cooperation for the accomplishment of this work.

ABSTRACT

Today, Electric vehicles (EV) are an interesting current and future option helps to reducing environmental impact by decreasing emissions and greenhouse gases. Electric vehicle face challenges related to safety, functionality, and operation. One of the key issues is the growing need for effective battery cooling to prevent potential thermal stability problems caused by extreme temperatures due to the traditional use of steel in battery enclosures. Letin Mengo (Anna 200) electric vehicle battery trays are made up of AISI 4031 steel materials that ensures the rigidity or solidity required to support the weight of an assembly of cells. However, steel has heavy weight, low thermal conductivities (TC) and high coefficient of thermal expansion (CTE) values that result in induced thermal stresses which can cause the device to fail permantly. This induces the overheating of the EV battery components, thermal stress and leads to reduce the overall efficiency of the battery's performance and life time.

Metal Matrix Composites are designed in order to have the combined properties of both metals and ceramics and have excellent mechanical and thermal properties. Due to its excellent thermophysical properties, including low coefficient of thermal expansion (CTE), high thermal conductivity, and improved mechanical properties, Al metal matrix reinforced by sic is used for heat-sensitive components. Therefore, the study focused on numerical analysis on thermal behavior of Aluminum Silicon Carbide (AlSiC) metal matrix composite materials for Anna 200 EV battery trays with cold plate cooling system. ANSYS work bench software are used to determine the surface temperature distribution of the EV battery tray.

According to the results, the AlSiC MMC material can reduce the maximum surface temperature from 83.47°C (for 4130 steel) to 69.64°C. Additional temperature reduction is possible with the help of liquid cooling system and this can maintain the battery tray surface temperature at around 33.1°C. In addition, result shows that the cooling system can safely maintain the battery surface temperature at a discharge rate of up to 3 C. in the explicit dynamic analysis the deformation and equivalent (von misses) stress of AlSiC tray is less than the convectional steel4130 EV tray.

Key Words: AlSiC**, CTE, TC, State of charging, Cooling, Surface temperature.**

LIST OF FIGURES

Figure 1. A) Anna 200 EV bottom battery tray and b) components of battery housing of Hyundai EV 2
Figure 2. The components inside an EV 3
Figure 3. Components of EV battery enclosure 5
Figure 4. Classification of composites based on matrix 8
Figure 5. A) AlSiC /CuSiC Thermoelectric cooler base with highly pyrolytic graphite (b) AlSiC liquid cooled aircraft power module base. 15
Figure 6 a). AlSiC Power substrates and IGBT basses and coolers, b) AlSiC power substrate in foreground with assembled power amplifier in background. 16
Figure 7. Phase of temperature rises in the battery cell [24]. 17
Figure 8. Thermal runaway flow chart [25]. 18
Figure 9. Classification of battery thermal management techniques [27]. 20
Figure 10. BTMS using air cooling system [28] 22
Figure 11. Battery liquid cold plate 24
Figure 12. Schematic of conventional heat pipe tubular structure with sealed ends 25
Figure 13. 43Ah electric motor battery back configuration 27
Figure 14. Actual picture of Letin mengo (Anna 200) electric vehicle battery pack 30
Figure 15. Placement of Letin mengo (Anna 200) electric vehicle lithium-ion battery pack 33
Figure 16. Thermal model setup[6]. 34
Figure 17. Experimental data for equivalent internal resistance and state of charge (SOC-) at 3C rate and 25℃ ambient temperature for IFR32135-15Ah battery cell. Via {HEFEI GUOXUAN high - tech power energy co., Ltd manufacturers}. 38
Figure 18. A) table indicates 3C SOC discharging analytical values of heat flux and heat generation rate of the battery b) graph represents the relationship between heat generation and DOD at 25℃ ambient temperature. 41
Figure 19. typical configuration of 150Ah Letin mengo (Anna 200) electric vehicle battery pack 44

Figure 20. Steps used on mechanical workbench 46
Figure 21. 3D solid work modeling of Letin mengo (Anna 200) electric vehicle battery tray 48
Figure 22 meshed model of the studied EV battery tray 49
Figure 23. Applied heat flux on the battery tray surface at 5% SOC discharge and 25℃ ambient temperature. 50
Figure 24. Mesh convergence test 51
Figure 25. Temperature contour of the entire battery tray in steel4130 material at 3C discharge and 25℃ ambient temperature. 53
Figure 26. Temperature contour of the entire battery tray in alsic MMC material at 3C discharge and 25℃ ambient temperature. 54
Figure 27. A) surface temperature distribution of EV battery tray under 95%and 50% SOC discharging a) using steel4130 b) using alsic MMC materials 56
Figure 28. Liquid cold plate for Letin mengo (Anna 200) electric vehicles battery pack 59
Figure 29. EV battery tray with cold plate 60
Figure 30. Temperature contours of the battery tray in alsic housing with cold plate a) under 5% SOC and b) under 95% SOC discharging. 61
Figure 31. directional deformation of a) steel4130 materials and b) Aluminum silicon carbide composite (AlSiC) material EV battery Tray. 64
Figure 32. equivalent (von misses) stress of a) steel4130 materials and b) Aluminum silicon carbide composite (AlSiC) material EV battery Tray 65

LIST OF TABLES

Table 1Properties of traditional and advanced electronic packaging materials[11] 9
Table 2 Properties of Al and SiC [13]. 11
Table 3 composition of aluminum used as matrix material (wt.%) 12
Table 4 The chemical composition of the AA6351 aluminum alloy. 12
Table 5 Effect and cause of operating battery cell at different temperature [26], [27]. 19
Table 6 materials used for battery tray in different EVs [31]. 29
Table 7 properties of AlSiC composites [23]. 32
Table 8 specification of 15Ah battery (for single battery) 45
Table 9 thermo physical properties of steel4130 and AlSiC materials used in the simulation ... 47
Table 10. Analytical calculated heat flux value at different SOC discharge and at 25℃ ambient temperature. 55
Table 11. Surface temperature of battery tray under different SOC discharging 57
Table 12. Specification of the liquid cold plate 59
Table 13 maximum deformation of different material EV battery Tray 64

LIST OF ABBREVIATIONS

EV	Electric Vehicle
MMC	Metal Matrix Composite
Alsic	Aluminum Silicon Carbide
CTE	Coefficient of Thermal Expansion
TC	Thermal Conductivity
FEA	Finite Element Analysis
BTMS	Battery thermal management system
SOC	state of charge
DOD	depth of discharge

TABLE OF CONTENTS

Contents

ACKNOWLEDGEMENT i
ABSTRACT ii
LIST OF FIGURES iii
LIST OF TABLES v
LIST OF ABBREVIATIONS vi
TABLE OF CONTENTS vii
CHAPTER ONE 1
INTRODUCTION 1
1.1 . Background 1
1.2. Battery System in An Electric Vehicle 3
1.3. General EV Battery Tray Material Performance Requirements 4
1.4. Battery Cooling System in Letin Mengo (Anna 200) Electric Vehicles 5
1.5. Statement of the Problem 5
1.6. Objectives 6
1.6.1. General Objectives 6
1.6.2. Specific Objectives 6
1.7. Significance of the Study 7
1.8. Scope of the Study 7
1.9. Methodology 7
CHAPTER TWO 8
LITERATURE REVIEW 8
2.1. Composites 8
2.2. Metal Matrices Composites (MMC) 9
2.2.1. Aluminum Metal Matrices Composites (ALMMC) 10
2.3. Silicon Carbide Reinforcement (SiC) 10
2.3.1. Aluminum Silicon Carbide Composites (AlSiC) 11

2.4. Mechanical Properties of Aluminum Silicon Carbide Composites (AlSiC) 11
2.5. Thermal Properties of Aluminum Silicon Carbide Composites (Al/sic) 13
2.6. Application Area of Aluminum Metal Metrics Composites (AlMMCs) 14
2.7. Effect of Temperature on EV Battery Cells 16
2.7.1. Effect of Low Temperature 16
2.7.2. Effect of Elevated Temperature 17
2.8. Battery thermal management system 19
2.8.1. Battery Thermal Management System (BTMS) Based on Various Cooling Methods 20
2.8.1.1. Medium used 21
2.9. Studies on The EV Battery Thermal Management 26
2.10. Research Gap 28
CHAPTER THREE 29
MATERIALS AND METHODS 29
3.1. Materials For Battery Tray 29
3.1.1. EV Battery Tray Datasheets 29
3.1.2. Selected Material for Anna 200 EV Battery Housing 31
3.2. Numerical analysis of electric vehicle (EV) battery tray 32
3.2.1. Battery Tray Configuration 32
4.2.2. Battery Tray Thermal Model 33
4.2.2.2. Convective Heat Transfer Coefficient 41
4.2.3. FEA Modeling and Analysis Method 44
4.2.4. Thermal Modelling of Battery Tray on ANSYS Workbench 45
4.2.4.1. ANSYS Transient Thermal Setup 47
4.2.4.2. Mesh Convergence Test 51
CHAPTER 4 52
RESULT AND DISCUSSION 52
4.1. Simulation of Surface Temperature of Battery Tray in Natural State 52
4.1.1. Simulation with steel 4130 materials 52
4.1.2. Simulation with alsic MMC materials 54

4.2. Effect of Different SOC Discharging in (3C-Rate)..... 55
4.3. Numerical Analysis of Cooling System Impact on Battery Thermal Management..... 58
4.4. Impact simulation of EV Battery Tray..... 63
4.4.1. Deformation..... 63
4.4.2. Equivalent(von-misses) stress..... 64
CHAPTER FIVE 66
CONCLUSION AND RECOMMENDATION..... 66
5.1. Conclusion..... 66
5.2. Recommendation..... 66
REFERENCES 67
APPENDIX..... 71

CHAPTER ONE

INTRODUCTION

1.1. Background

Electric vehicles (EVs) represent a promising current and future alternative to the gradual replacement of traditional combustion engine vehicles, offering several environmental benefits such as reduce emissions of greenhouse gases and pollutants [1].

The power source of electric vehicles is from various batteries, such as lead-acid battery, lithium-ion battery, and nickel-metal hydride (Ni-MH) battery, and the performance of the battery greatly affects the performance of electric vehicles. The energy source of Letin mengo electric vehicles (Anna 200) is Li-ion batteries. Lithium-ion barriers are considered the main option for energy storage in electric and hybrid vehicles. The battery offers higher performance and specific energy than lead-acid batteries and nickel-metal hydride (Ni-MH) batteries. They are characterized by high energy density, low self-discharge rate, no memory effect and small dimensions [2].

Anna 200 electric vehicles have battery tray designed in strong interaction with the design of the car and which consists of lower tray integrated with compartment for battery module without cooling plate. The primary function of the battery tray is to provide mechanical and thermal interfaces to the vehicle. In addition, the battery tray serves as a safety cage in the event of impacts, protecting the battery from external impacts and at the same time helping to maintain thermal stability by dissipating heat to the environment [3]. High temperatures in the battery tray can significantly reduce material performance, leading to problems such as melting and potential burning of packaging materials [4]. In the automotive industry, components exposed to high heat require materials with exceptional thermal shock resistance that can maintain their strength at extremely high temperatures without any loss of performance [2].

EV battery tray must be dissipating the heat effectively during charging and discharging process. The battery tray materials should have high thermal conductivity (TC) and low coefficient of thermal expansion (CTE) with good mechanical strength and these can be achieved by combining the properties of two or more materials [5].

MMC composite has been established as highly efficient, high performance structural materials and the composites are usually used for precisely optimizing the properties of the material which provides combination of mechanical properties such as tensile modulus, compressive strength and impact strength.

Aluminum metal matrix with ceramic reinforcement composites such as Silicon Carbide, Aluminum nitride, Aluminum Oxide and silicon nitride are used in having extremely vast applications in aviation, mechanical, electrical, automotive, electronics and transport industries. From those AlMMC, Al/sic are the most common MMC used in different housing application such as for Thermoelectric cooler base/cover, liquid cooled aircraft power module base [4].

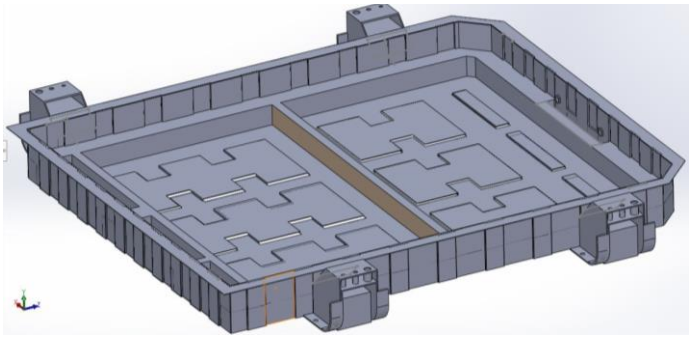

A)

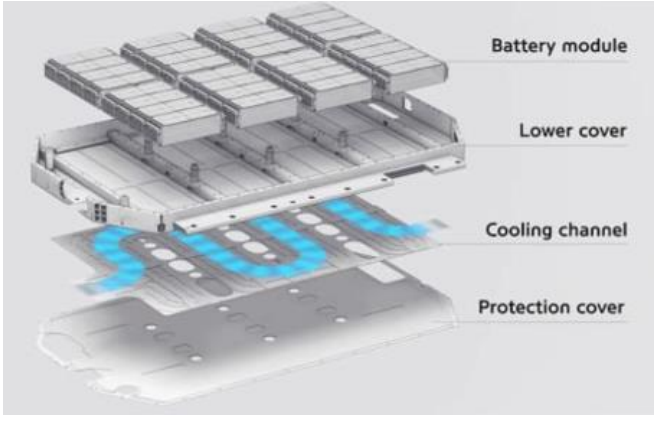

B)

Figure 1. A) Anna 200 EV bottom battery tray and b) components of battery housing of Hyundai EV

1.2. Battery System in An Electric Vehicle

Battery cells are assembled into a single mechanical and electrical units known as battery modules. These modules are electrically connected and form a battery that serves as a power source for the electronically controlled system. In electric vehicles, the battery pack is designed to closely integrate with the design of the car and includes different components of the car such as converter and electric motors.

The battery system increases the energy efficiency of electric vehicles by providing high energy density and enabling rapid acceleration. It also significantly helps minimize environmental impact by producing zero emissions and reducing greenhouse gases.

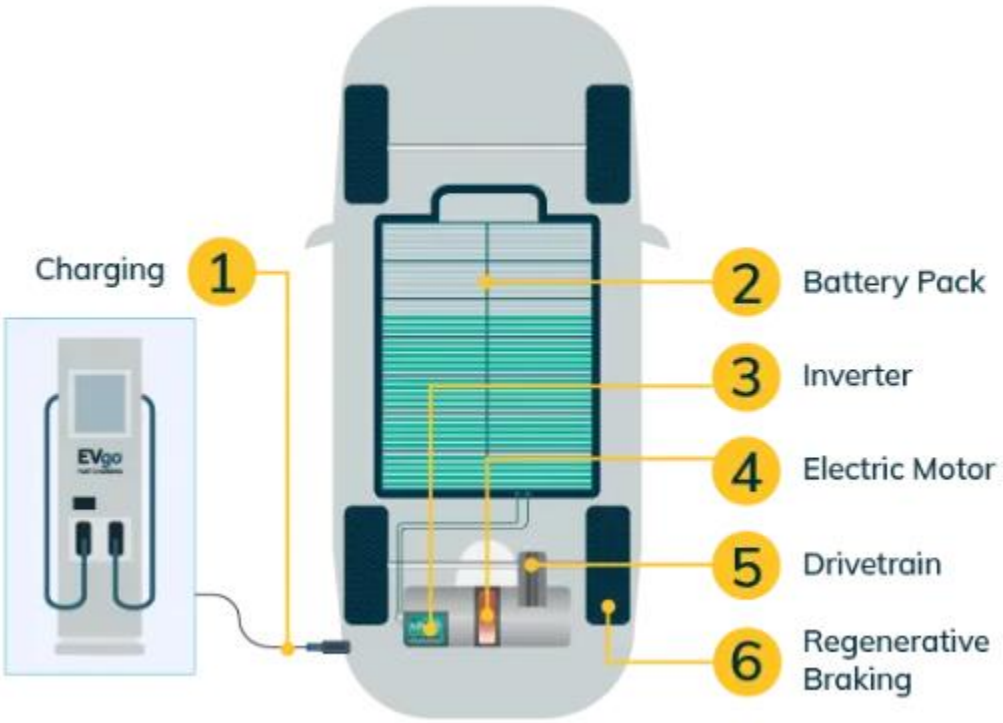

Figure 2. The components inside an EV

1.3. General EV Battery Tray Material Performance Requirements

EV battery pack should be

- Light weight
- Thermally stable
- Effective support to the battery module (low deformation)
- Impact resistance
- More resistant to dynamic loads (vibration)
- Wear resistance
- Resist corrosions
- Low manufacturing cost
- Structurally stable
- Easy to manufacture

This research focuses on improving the thermal stability of the EV battery trays, which is critical to prevent overheating, increase battery efficiency, and extend battery life. To achieve this, I replaced the conventional steel materials with AlSiC (aluminum silicon carbide), a material known for its high thermal conductivity and excellent heat dissipation. This change is enhanced to significantly improve overall battery temperature management.

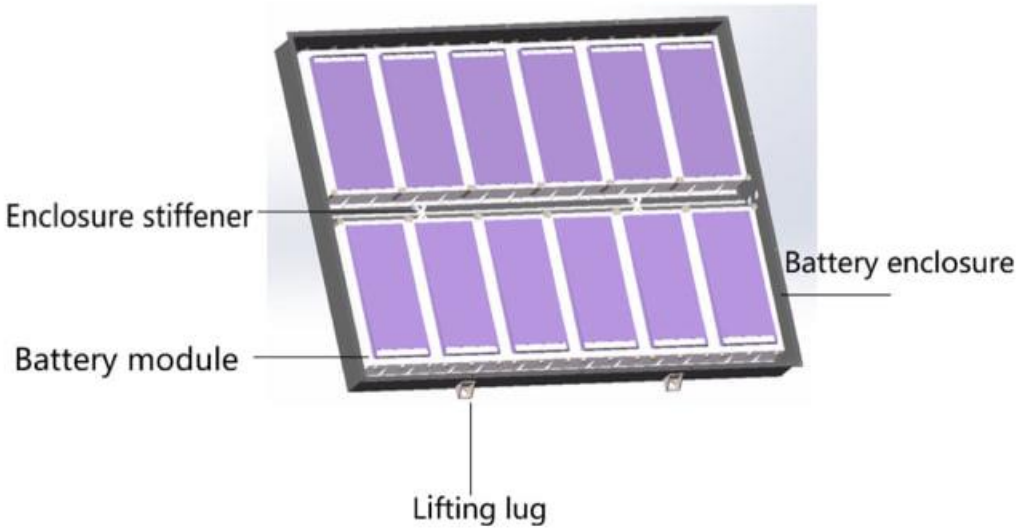

Figure 3. Components of EV battery enclosure

1.4. Battery Cooling System in Letin Mengo (Anna 200) Electric Vehicles

Electric Vehicles have mechanisms to cool their batteries and Letin mengo (Shangan Anna 200) EV has no cooling components inside the battery to reduce the temperature. A method utilized is directing air flow over the steel battery case while the vehicle is in motion and charging. The steel battery tray has a breather that used to remove the hot air in to the surrounding from the battery package when the temperature increased in the battery cell. If the batty cell temperature is above **60**℃ the thermal management system may will have locked and stop the car. The air-cooling systems in Anna 200 should be keep the battery pack in the temperature range of about **-30 to 60** degrees Celsius.

1.5. Statement of the Problem

The use of MMC materials has greatly expanded in recent decades due to their excellent mechanical and thermal properties. These include high strength, low density, excellent stiffness and toughness, corrosion resistance, fatigue resistance, low creep, minimal wear and high thermal conductivity compared to unreinforced alloys.

Metal Matrix Composite has been established as highly efficient, high performance structural materials and AlSiC are the most common MMC used in different applications that need thermal stability like heat sink ,electronics cover and also for applications that needs improved mechanical properties [4].

The battery tray for the Letin Mengo electric vehicle (Anna 200) are made of AISI 4031 steel, which provides the necessary rigidity to support the weight of the cell assembly. However, steel is heavy has around 7850 kg/m^3 density, has a low thermal conductivity (42.5 W/m℃) and exhibits a high coefficient of thermal expansion (12.2$\mu m/m$℃). These properties can lead to thermally induced stresses that can compromise the integrity of the device. As a result, internal components can overheat, causing thermal stress that reduces overall efficiency and battery life [6].

Letin Meng (Anna 200), an electric car uses ambient air to cool the battery during charging and discharging process. Research has shown that even at high airflow rates, air cooling may not adequately address the heat dissipation requirements of an EV battery during these processes in

hot conditions. The low thermal conductivity of the air can further complicate the cooling of the battery block at elevated temperatures [7].

So, in order to fix this problem MMC materials are one of the materials which are attracting and being solutions of such problems. AlSiC composites have a unique properties of the light weight, high strength, high specific modulus, high fatigue strength, good impact strength and good thermal conductivities [4].

One of the biggest challenges for extending the life of electric car batteries is maintaining the stability of the surface temperature of the battery. So, to use AlSiC composite material for battery tray with battery cooling system for such specific application, the heat dissipation of the materials and effect of battery cooling systems are investigated. This study conducts numerical analysis of the thermal performance of AlSiC MMC with cold plate for Anna 200 electric vehicle battery tray applications.

1.6. Objectives

1.6.1. General Objectives

The main objective of this study is to analyze the thermal behavior of Aluminum Metal Matrix Composite (Al MMC) as optional battery tray materials with an adequate cooling system for Letin mengo (Anna 200) electric vehicle application.

1.6.2. Specific Objectives

The specific objectives of this study include:

- To analyze the thermal performance of the EV battery tray with currently in use material (steel 4130).
- To analyze the thermal performance of the EV battery tray with a high thermal conductivity material (alsic MMC).
- To identify the effect of SOC discharging in (3C-Rate) under different depth of discharge (DOD) on the Letin mengo (Anna 200) electric vehicles Li-ion battery tray.
- analyzing stress and deformation in EV battery tray

1.7. Significance of the Study

The benefit of this study is analyzing thermal behavior of aluminum silicon carbide (AlSiC) metal matrix composites with an appropriate cooling system to get better thermal stability for Letin mengo (Anna 200) electric vehicles Li-ion battery pack. This can give dimensional stability under variable temperature working condition, reduced thermal stress and good heat dissipation through battery pack.

1.8. Scope of the Study

In this study, the thermal behavior of an aluminum silicon carbide (AlSiC) metal matrix composite material for electric vehicle battery tray applications is analyzed using the finite element method (FEM). The analysis includes the change in battery tray materials and state of charge (SOC) during discharge of lithium-ion batteries. No experimental investigations are performed in this study; instead, relevant data from previous experiments will be used.

1.9. Methodology

First, the research began by reviewing various literatures and collecting relevant data from an environmental technology green tech company. This included detailed information on the battery tray material, accurate direct measurement of the battery, battery compartment dimension, and specifications of the battery system used in the EV. These comprehensive data sets formed the basis for subsequent modeling and analysis.3D modeling of the EV battery tray was developed using SOLIDWORK 22.0 software. The model was used as an input step file to simulate the thermal performance of the battery tray material under operating conditions. Simulation and finite element analysis were performed using ANSYS Workbench 21.0 software. The analysis focused on evaluating the surface temperature distribution of the battery tray with steel4130 and AlSiC materials and explicit dynamic analysis with these two materials.

CHAPTER TWO

LITERATURE REVIEW

2.1. Composites

Composites are a physical mixture of two or more different materials in which the mixture gives better material properties than those of any one of the materials.

A composite consists of three components:

I. The matrix serves as the continuous phase. It is a more ductile and less hard component that binds all the parts of the composite together, holding the stiffeners in place and distributing the load between them.

II. Reinforcements act as a discontinuous or dispersed phase that includes fibers and particles. This phase is usually stronger than the matrix, it is sometimes called "reinforcement phase" and serves to increase the strength of the composite.

III. The fine interphase region, also known as the interface; it separates the fiber and matrix

Based on matrix materials composite materials are classified as follow[7].

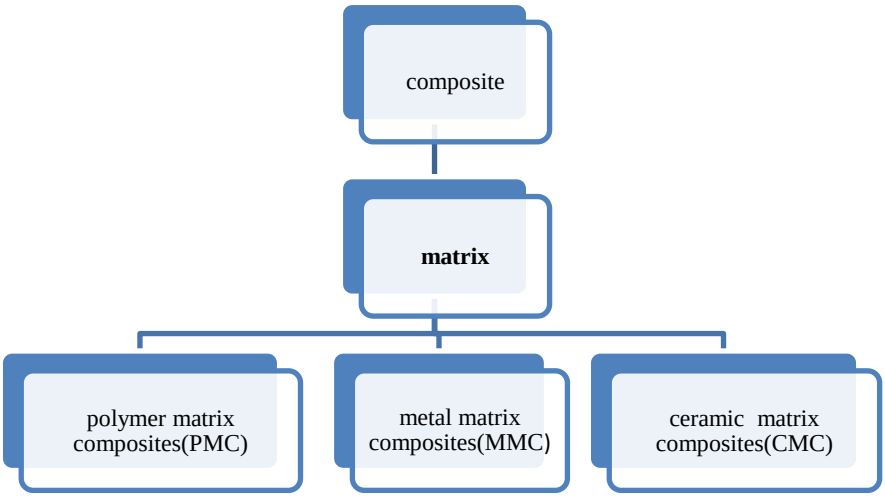

Figure 4. Classification of composites based on matrix

2.2. Metal Matrices Composites (MMC)

Metal matrix composite materials, created by combining two or more materials, which offers a distinct advantage over organic matrix composites. These composite consists primarily of a metallic substance, mostly magnesium, aluminum, titanium, cobalt, and copper, coupled with ceramics (carbides and oxides) or metallic (tungsten, molybdenum) phases [8].

Metal Matrix Composites (MMC) are designed to integrate the advantageous properties of both metals and ceramics. Compared to polymer matrix composites, they exhibit superior mechanical and thermal properties, including higher strength-to-density and stiffness-to-density ratios, improved fatigue resistance, increased strength at elevated temperatures, reduced creep rates, lower coefficients of thermal expansion (CTE), and improved durability against wear [9].

The mechanical and thermal properties of the Metal Matrix composites depend on many factors such as matrix material, weight fraction, reinforcement phase material and the production method of the composite.[10]

Table 1Properties of traditional and advanced electronic packaging materials[11]

Reinforcement	Matrix	Thermal conductivity(W/m.K)	CTE (ppm/K)	Density ($g.cm^{-3}$)
-	Copper	400	17	8.9
-	Aluminum	218	23	2.7
-	Copper/Tungsten	157-190	5.7-8.3	15-17
-	Kovar	17	5.9	8.3
Sic	Aluminum	170-220	6.2-16.2	3.0
Sic	Copper	320	7-10.9	6.6
Diamond	Aluminum	550-600	7.0-7.5	3.1
Diamond	Copper	600-800	5.8	5.9

2.2.1. Aluminum Metal Matrices Composites (ALMMC)

Aluminum is a widely available and commonly used metal that is easy to work with, lightweight, and offers good corrosion resistance, strength, and high thermal conductivity at a low cost. However, its performance at elevated temperatures is limited due to its low melting point, hardness, and wear resistance. In addition, aluminum has high coefficients of thermal expansion (CTE), which requires the use of materials that can compensate for thermal stress. This can lead to thermally induced stresses that can result in device failure [9].Aluminum metal also has low corrosion resistance, low ultimate bending strength, also have low wear resistance We used reinforcing materials to enhance the existing properties of aluminum and its alloys such as the tensile strength, melting temperature, thermal stability and mechanical characteristics.

The material embedded to aluminum/aluminum alloy porous matrix layer and serve as reinforcement, which is usually a nonmetallic and commonly ceramics such as Silicon Carbide, Aluminum nitride, Aluminum Oxide and silicon nitride. And also Properties of AlMMC can be varied by varying the composition of constituents and their volume fractions [12].

2.3. Silicon Carbide Reinforcement (SiC)

Silicon carbide is a widely used structural ceramic known for its excellent mechanical properties, including low density, excellent wear resistance, high strength and excellent hardness. It is a cost-effective material with a high modulus of elasticity, making it ideal for use as a reinforcing phase. Compared to silicon nitride, the raw materials for the production of silicon carbide are more readily available, resulting in lower production costs than those associated with tungsten carbide [12].

Table 2 Properties of Al and SiC [13].

Property	**Aluminum**	**SiC**
Elasticity modulus	E_a=73 Gpa	E_s=450 gpa
Specific mass	γ_a=2800 Kg/m^3	γ_s=3200 Kg/m^3
Thermal dilatation coefficient	α_a=23.6x10^{-6} $^oc^{-1}$	α_s=4.0x10^{-6} $^oc^{-1}$
Poisson's ratio	μ_a=0.33	μ_s=0.17
Transversal elastic modulus	G_a=27.4 gpa	G_s=192 gpa

2.3.1. Aluminum Silicon Carbide Composites (AlSiC)

Al-SiC is a metal matrix composite consisting of an aluminum matrix and silicon carbide as the reinforcement phase. The addition of silicon carbide particles to the pure metal enhances the mechanical properties tensile strength, hardness and wear resistance of the composites [12].

Reinforcements such as silicon carbide (SiC) increase the strength, creep resistance, and modulus of elasticity of aluminum, but tend to decrease its fracture toughness, thermal conductivity, and coefficient of thermal expansion (CTE). However, aluminum-silicon carbide (AlSiC) composites retain high thermal conductivity, comparable to pure aluminum, and provide better reliability by preventing deformation or bending of the package and substrate materials. Traditional electronic packaging materials such as Kovar and Fe-Ni alloys, which have lower thermal dissipation, can lead to delamination, air gaps and potential failures. In contrast, AlSiC metal matrix composite (MMC) motherboards can withstand thousands of thermal cycles without delamination between the substrate and the motherboard [4].

2.4. Mechanical Properties of Aluminum Silicon Carbide Composites (AlSiC)

Md. H. Rahman et al. Studied the effect of silicon carbide (SiC) reinforcements in Al matrix composites on Microstructures, Vickers hardness, tensile strength and wear performance of the composites. They prepared aluminum metal matrices composites of (0, 5, 10 and 20 wt. %) sic content by using stir casting fabrication technique.

Table 3 composition of aluminum used as matrix material (wt.%)

Elements	Fe	Si	Mn	Cu	Mg	Al
%	0.16	0.19	0.01	0.01	0.01	Balance

The result indicated that porosity is observed in the micro structure of AlSiC composites. Addition of sic in Al matrix increased wear resistance, hardness and tensile strength of composites and 20 wt. % content of sic have maximum wear resistance, hardness and tensile strength [14].

V. Mohanavel et al. Examined the influence of sic addition on AA6351 aluminum matrix composites by using stir casting fabrication technique and the prepared composites were examined by using an optical microscope. Density, hardness, yield strength and impact strength of the composite were investigated. They were used sic content in aluminum matrix composite by varying from 0% to 20% in a stage of 4%.

Table 4 The chemical composition of the AA6351 aluminum alloy.

Elements	Si	Fe	Cu	Mn	Mg	Cr	Zn	Ti	Al
% By weight	1.0	0.60	0.10	0.5	0.7	0.25	0.10	0.20	Remaining

The result shows in optical microphotographs uniform distribution of sic particles have a good bonding between the matrix alloy and sic reinforcement. Hardness, yield strength and impact strength of the composites are changed with in different weight fraction of sic reinforcement. The density of the AlSiC composites was increased from 2.69 to 2.796 gm/cm3 with respect to inclusion of wt.% of sic particles from 0 wt.% to 20 wt.% [15].

Kada. Z et al. Investigated the dynamic response of functionally graded silicon aluminum carbide (FGM) materials subjected to impact loading by projectiles simulating fragments. They also validated the elastoplastic impact modeling of FGM using dynamic finite element analysis using SCM and dynamic Tamura-Tomota-Ozawa (DTTO) models. The analysis used five different compound layers and the results showed that the exponent of the compound gradient significantly affected the impact response. The projectile's kinetic energy was absorbed by the plate as plastic strain energy, with the ceramic-rich layers exhibiting poor energy absorption. The linear

distribution of functionally graded layers improved ballistic performance, improved dynamic behavior and increased both compressive strength and energy absorption capacity [16].

K. Karvanis et al. Examined Mechanical properties of AlSiC metal matrix composites, such as tensile and compressive strength, hardness, and impact strength, were investigated to determine the optimal silicon carbide content. Scanning electron microscopy was used for analysis. The results showed that a higher proportion of silicon carbide improved the tensile and compressive strength of the composites. Additionally, increasing the sic content resulted in greater hardness, but also reduced the overall displacement and overall energy absorption during impact tests [10].

2.5. Thermal Properties of Aluminum Silicon Carbide Composites (Al/sic)

K. A. R. Kumar et al. Analyzed temperature dependent material properties and thermal, stress and deformation numerical aspects and various physical, metallurgical properties of the aluminum silicon carbide (AlSiC) composites using finite element (FE) matrix formulation. The result showed increasing the volume fraction of sic in aluminum matrix results linearly decreasing in coefficient of thermal expansion (CTE). The SiC is the main factor contributing to the CTE of MMC and thermal stress and deformation is increased with increasing temperatures [17].

M. Z. Bukhari et al. Developed, study and characterize a new material in order to get excellent thermo-physical properties such as low coefficient of thermal expansion (CTE), high thermal conductivity and improved mechanical properties such as higher specific strength, better wear resistance and specific modulus. According to their findings MMCs of AlSiC have an improve properties in thermal conductivity as well as in coefficient of thermal expansion (CTE), are now the possible solution for electronic packaging industry [4].

P. Van Trinh et al. Investigated the microstructure, mechanical properties, and wear behavior of oxidized-sicp/Al6061 composites by fabricated the composites using a spark plasma sintering technique and oxidizing-silicon carbide particle 10% by weight added in Al6061at 1200°C,1300°C and 1400°C.the result showed that the interfacial binding intensity between Al6061 and oxidized sicp was improved. Oxidized sicp, in a composite improved the hardness, the ultimate tensile strength and elongation by 75%, 26 % and 32% respectively and the coefficient of friction and

specific wear levels for composites oxidized by SiCp/Al6061, respectively, have been lowered by 7% and 17 %. This improved hardness and strength of AlSiC [18].

R. Zare, H. Et al. Investigated the effect of different mass percentages of sic reinforcing particles on the physical and thermal properties of the Al matrix composite (6061). Composite powders with different levels of reinforcement were prepared by hot pressing. Dilatometric tests revealed that an increase in SiC content led to a decrease in the coefficient of thermal expansion. Moreover, as the SiC content increased, the thermal conductivity decreased due to the increase of crystalline defects at the phase interfaces [19].

S. Sarapure, et al. Studied statistical behavior of the corrosion AlMMCs by using a Taguchi method and for the fabrication, the Stir casting technique was adopted in which Al6061 reinforced by sic with 0 percent, 2 percent and 4 percent weight. Research results have shown that composite materials exhibit significantly better corrosion resistance compared to monolithic 6061 alloys. Studies have shown a significant reduction in corrosion rate and weight loss per unit area over time. In contrast to the unreinforced monolithic matrix alloy, AlMMCs showed improved corrosion resistance [20].

T.H. Nam et al. Studied the coefficient of thermal expansion of aluminum metal matrix with densely packed silicon carbide particles between 20^{o}c to 500^{o}c using finite element analysis (FEA)based on two-dimensional unit cell model. They analytically calculated the physical coefficient of thermal expansion (CTE) of the Aluminum Metal Matrix composite reinforced with 70 wt. %. Of sic particles to identify discrepancies in experimentally obtained thermal expansion properties. The results showed that the thermal expansion behavior of the composites is significantly affected by the presence of voids and the experimental values are in good agreement with the physical CTE values [21].

2.6.Application Area of Aluminum Metal Metrics Composites (AlMMCs)

Aluminum Metal Matrix Composites (AlMMCs) are considered innovative materials for numerous engineering applications, holding significant potential in generating composites with specific properties tailored for various uses through the incorporation of a diverse range of reinforcing materials. AlMMCs possess good characteristics in the comparison of traditional

materials, which includes, excellent mechanical properties and having extremely vast applications in aviation (such as aircraft, helicopters and other large aircraft wings, rudders, flaps, fuselage), mechanical, electrical, automotive (such as for piston ring for the engine, connecting automotive drive shafts, rocker arms, chassis and disk break), electronics (electronic packages and covers) and transport industries [9].

Aluminum Metal Matrix Composites (AlMMCs) used for its good mechanical and thermal properties such as strength, less density, excellent stiffness, lightweight, toughness, resistance to corrosion, fatigue, low creep and wear relative to non-reinforced alloy and high thermal conductivities. Due to this properties AlMMCs, suitable materials for many applications. It is commonly used in the aircraft, automobile, marine, leisure, telecommunications and electronics industries [22].

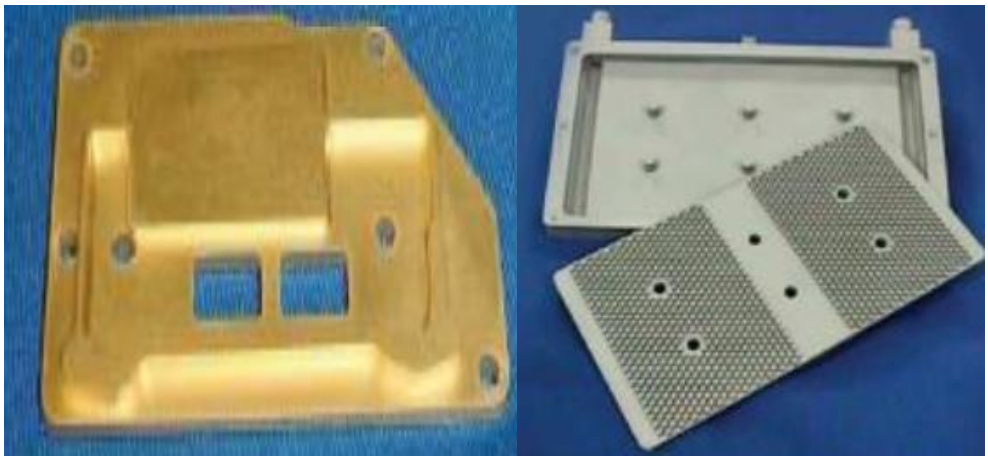

A) b)

Figure 5. A) AlSiC /CuSiC Thermoelectric cooler base with highly pyrolytic graphite (b) AlSiC liquid cooled aircraft power module base.

To improve thermal conductivity and coefficient of thermal expansion (CTE), AlSiC metal matrix composites (MMCs) have emerged as a viable solution for the electronic packaging industry. The Aluminum Silicon Carbide (AlSiC) material system offers package designers a unique set of properties that are ideally suited for creating high performance and advanced temperature controlled package designs [4].

Aluminum Silicon Carbide (AlSiC) metal matrix composites (MMC) has high thermal conductivity and low thermal expansion coefficient (TCE) values used to providing thermal management solutions for numerous electronics applications such as Flip Chip Lids, Optoelectronics Packaging, Power Devices and High Brightness LED applications [23].

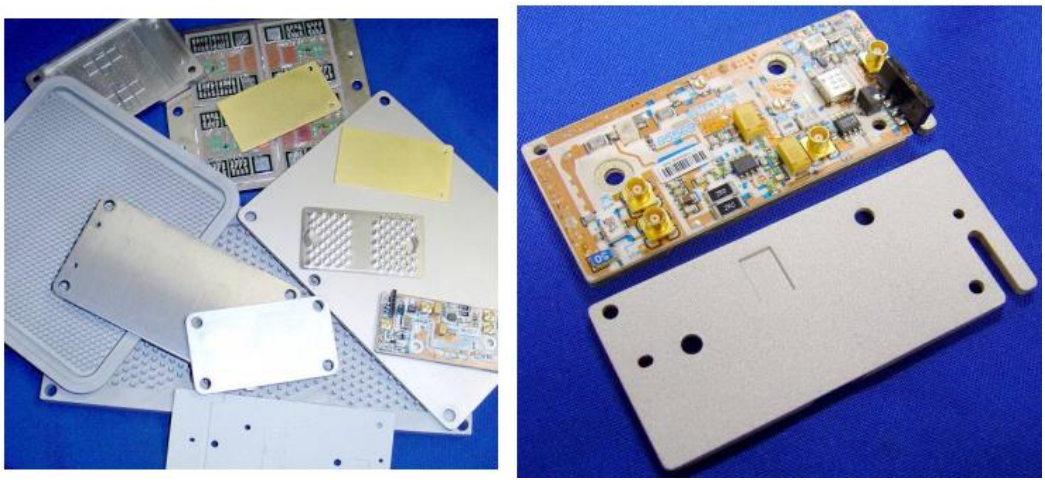

a) B)

Figure 6 a). AlSiC Power substrates and IGBT basses and coolers, b) AlSiC power substrate in foreground with assembled power amplifier in background.

2.7. Effect of Temperature on EV Battery Cells

Lithium-ion (Li-ion) batteries are defined by a complex series of physio-chemical processes and are classified as temperature-sensitive devices, with their performance and safety significantly affected by temperature fluctuations. Numerous studies have shown that lithium-ion batteries work most efficiently at temperatures close to an ambient temperature of 25℃.

2.7.1. Effect of Low Temperature

Different researches indicated that in constant current discharge/charge test of Lithium ion (Li-ion) batteries, the usable battery capacities loss increase as the operating temperature decrease .the poor performance of Lithium ion (Li-ion) battery cells at low temperature due to the lower electrolyte conductivity which affects Li-ion transportation rate between two electrodes at these temperature and Further researches suggested that lack of electrode activity can also cause unsatisfactory performance of Li-ion battery.

2.7.2. Effect of Elevated Temperature

Temperatures above 40°C can lead to chemical decomposition in the battery cell and degradation of the lithium ions. This can adversely affect the performance of the Li-ion battery, resulting in a reduction in its ability to retain power and energy over time.

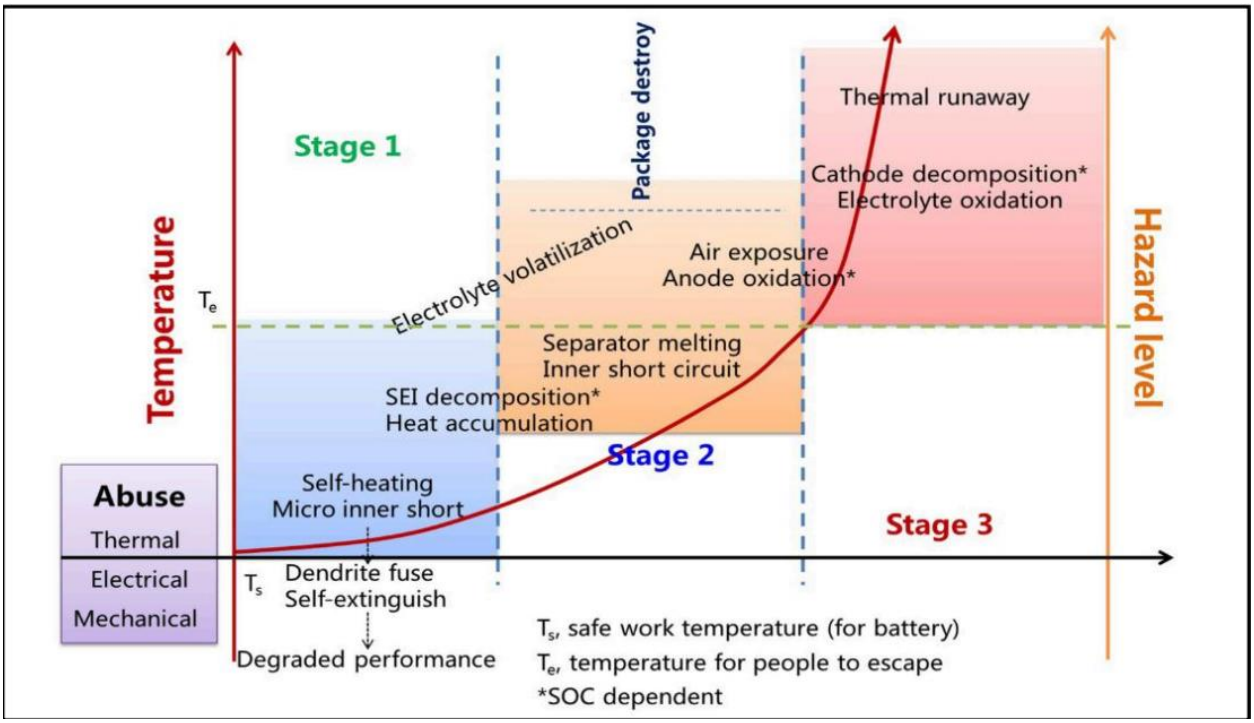

Figure 7. Phase of temperature rises in the battery cell [24].

Thermal runaway refers to the initiation of an exothermic chain reaction where the battery cells begin to spontaneously heat up at a rate exceeding 0.2°C per minute. This excessive heat production accelerates the self-heating process, which eventually leads to self-ignition of the battery's chemical materials. High temperatures associated with thermal runaway may cause the mounting brackets near the affected battery area to melt or vaporize. As a result, the battery may lose its original location. As the affected battery cell or module moves, the gaps between the battery components can shrink, which can reduce the resistance to the spread of thermal runaway [24].

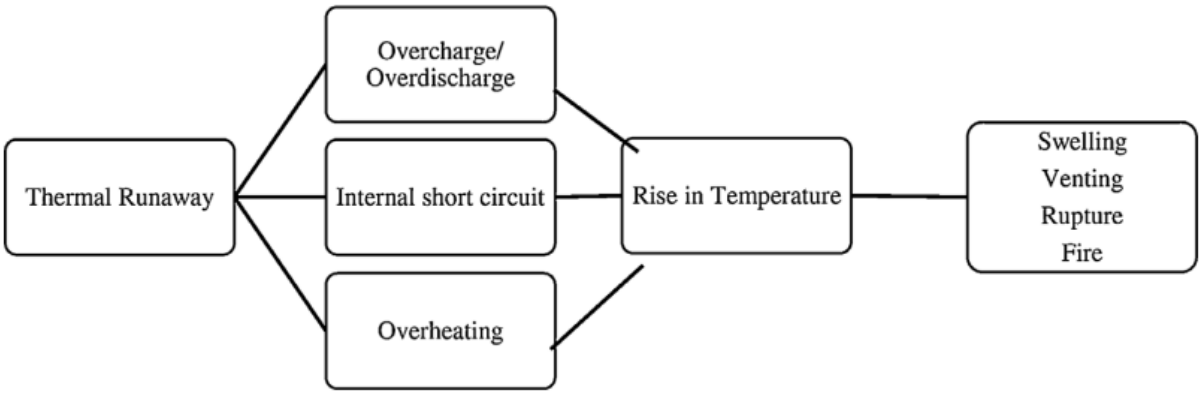

Figure 8. Thermal runaway flow chart [25].

Elevated surface temperatures of Li-ion batteries used in electric vehicles can lead to heat leakage, which reduces battery efficiency and causes a constant rise in temperature that can lead to fire. During the charging and discharging process, complex chemical reactions take place inside the battery, which generate maximum heat and cause a constant rise in temperature. If this heat is not dissipated quickly, thermal runaway can occur. As a result, the implementation of a Battery Temperature Management System (BTMS) is necessary to regulate the temperature of the battery to maintain optimal operating conditions and ensure the safety of electric vehicles [2].

Table 5 Effect and cause of operating battery cell at different temperature [26], [27].

Battery cell temperature	Cause	Leads to	Effect
High	Decomposition of Electrolyte	Permanent loss of lithium	Capacity loss
	Constant low-rate reactions	Increasing impedance	Power loss
	Reduction in the anode surface for li-ion intercalation	Increasing impedance	Power loss
	Binder Decomposition	Deterioration of mechanical stability	Capacity loss
25℃-40℃	Maximum cycle life		
15℃-24℃	Superior energy storage capacity		
Low	Plating of Lithium	Irreversible loss of lithium	Capacity or power fade
	Decomposition of Electrolyte	Electrolyte loss	

2.8. Battery thermal management system

Thermal safety is a critical concern in the research and development of power batteries for electric vehicles. Creating an efficient temperature management system for battery packs or modules is critical to improving battery life and reducing the overall cost of EVs. It is important for power batteries to operate within an optimal temperature range and maintain an even temperature distribution to save energy and reduce costs associated with electric vehicles [2].

Controlling the temperature of the battery and the environment in which the battery operates is critical to maximizing its energy capacity. For safe operation, it is recommended to keep the battery temperature below 50 °C (depend on battery types) [6]. Managing the large temperature rises and non-uniform thermal gradients across the battery pack is a major concern in the design of large battery packs essential for supporting an EV driveline [27].

2.8.1. Battery Thermal Management System (BTMS) Based on Various Cooling Methods

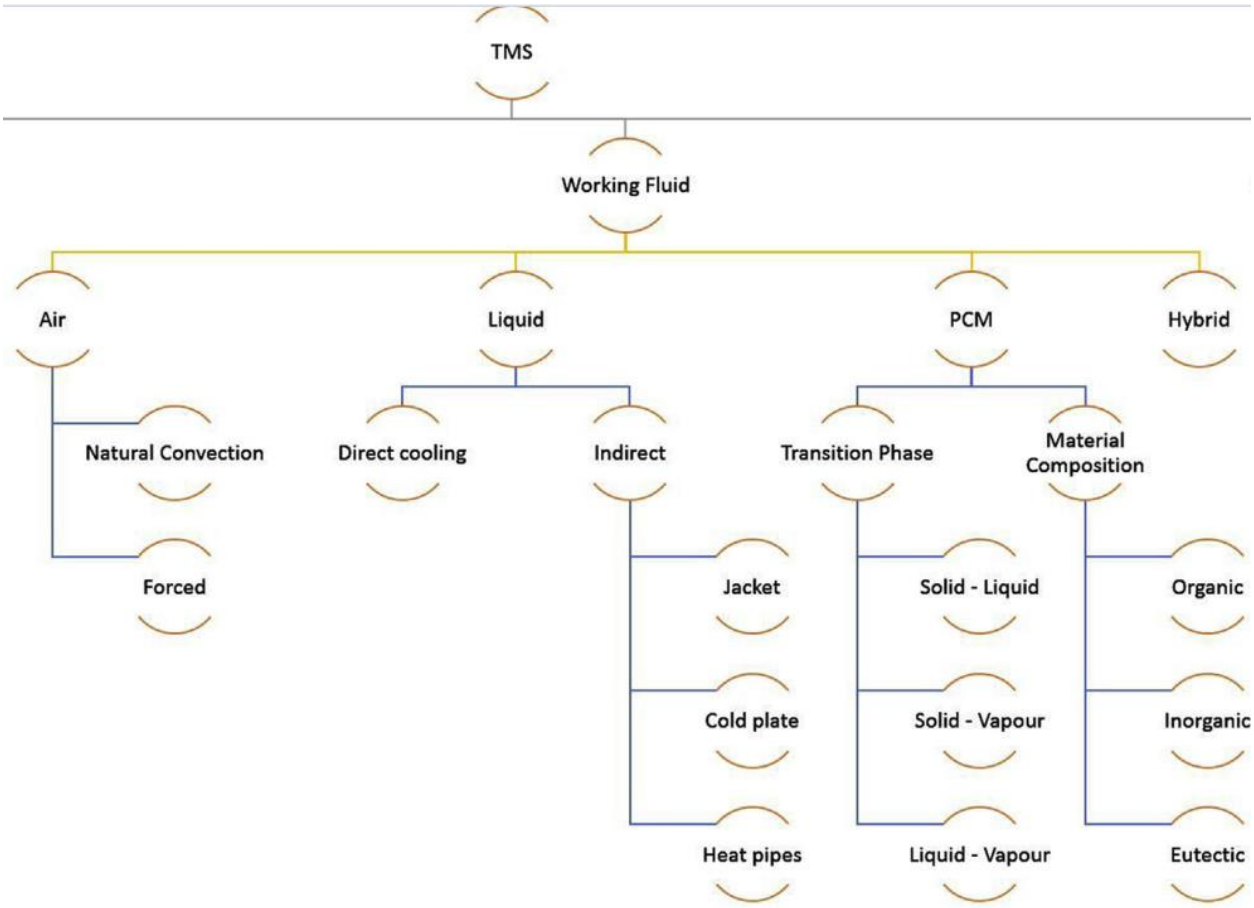

Figure 9. Classification of battery thermal management techniques [27].

2.8.1.1.Medium used

A battery thermal management system can be classified by the working fluid (medium used) used in the cooling loop. These are;

A) Air cooled

I. Free convection

II. Forced convection

B) Liquid cooled

I. Cold plate

II. Heat pipe

III. Jacket cooling system

C) phase change material

D)any combination of the above

A) Air cooling system (ACS)

Air-cooling system (ACS), where air is used as the cooling medium. Increasing the air-cooling rate will reduce the time it takes for the cell to reach steady state, minimizing the risk of overheating and thermal runaway. Air cooling can be done by natural convection and forced convection.

I. Free convection

The heat generated from the battery cell is removed in to the surrounding naturally without any help of external device such as fan.in this system there is no moving parts, noise and have low initial and maintenance costs but for high power components it is limited and less efficient to cool the hot surface.

II. Forced convection

In forced air-cooling system uses mechanical device such as fan, blowers to increasing the heat dissipation rate to move the air actively through the heat surface. When compared to free convection it is better for high power electronics or high heat dissipation application. It improves

convection, higher cooling capacity and the overall cooling efficiency.it is the simplest and cost-effective way of regulating the temperature of electric vehicles (EVs) battery pack.

However, with air-cooled thermal management systems, ambient air flows unidirectionally through the spiral, entering from one side and exiting from the opposite side. This unidirectional coolant flow often results in uneven temperature distribution, typically exceeding 5°C. In addition, the ambient air has a low thermal conductivity, which makes it difficult to effectively cool the battery at elevated temperatures [27].

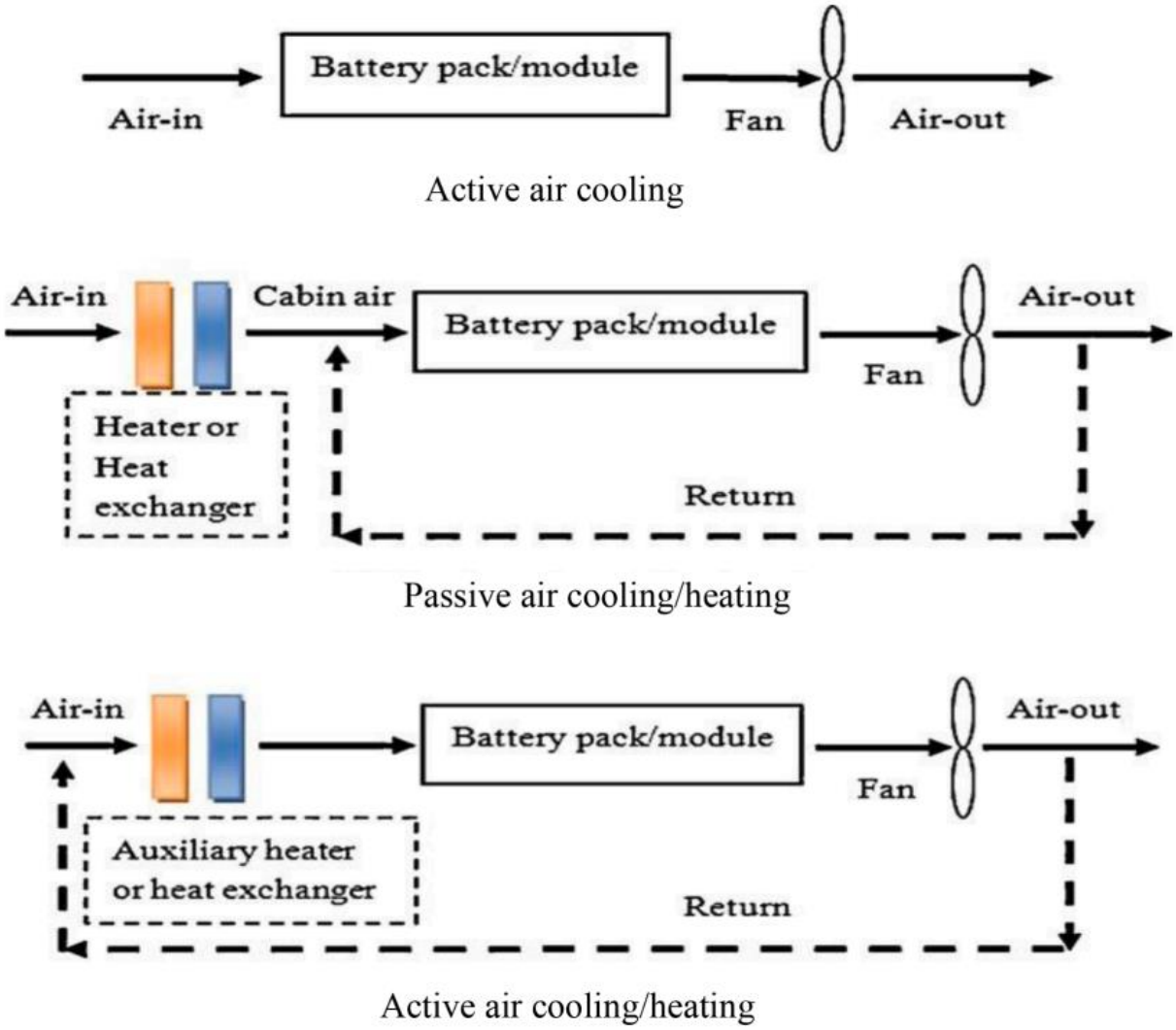

Figure 10. BTMS using air cooling system [28].

B) Liquid cooling system (LCS)

In a liquid cooling system (LCS), liquid serves as the cooling medium. Various studies have shown that even very high airflow rates may not be sufficient to meet the heat dissipation needs of electric vehicle battery packs during charging and discharging. An effective alternative to cooling battery packs is a liquid cooling system, which may involve circulating liquid through housings or tubes surrounding the battery pack or using liquid-cooled plates. In addition, liquid cooling systems can be designed using cold plates and heat pipes.

I. Cold plates

A cold plate is integrated directly to the heated components for liquid coolant to carry the heat from the hot component. The hot component would be in close contact with the cold plate which has internal channel or tube for circulating a coolant. The cold plate absorbs heat directly from the hot component and providing efficient cooling through the system. Cold plates are mostly preferred in electric vehicles (EV's) because of the strict space limitation.

In the case of thermal management system (TMS)liquid-cooled system using cold plate, the metal pressing is placed between adjacent battery cells and a heat transfer fluid is passed over these inbuilt channels. The liquid absorbs the entire remaining excess heat from the battery pack and transfer it into an external heat exchanger (HX) where it finally released into the surrounding environment [27].

Figure 11. Battery liquid cold plate

II. Heat pipe

Heat pipe thermal management is a passive system that uses a phase change of the working fluid in a sealed pipe. When heat is absorbed at one end of the pipe (the evaporator), the liquid evaporates and moves to the cooler end (the condenser). In the condenser, the vapor releases heat and condenses back into a liquid form, which is then returned to the evaporator by capillary action or gravity, creating a continuous cycle. This process works without the need for external power and relies only on a thermal gradient to transfer heat from one area to another.

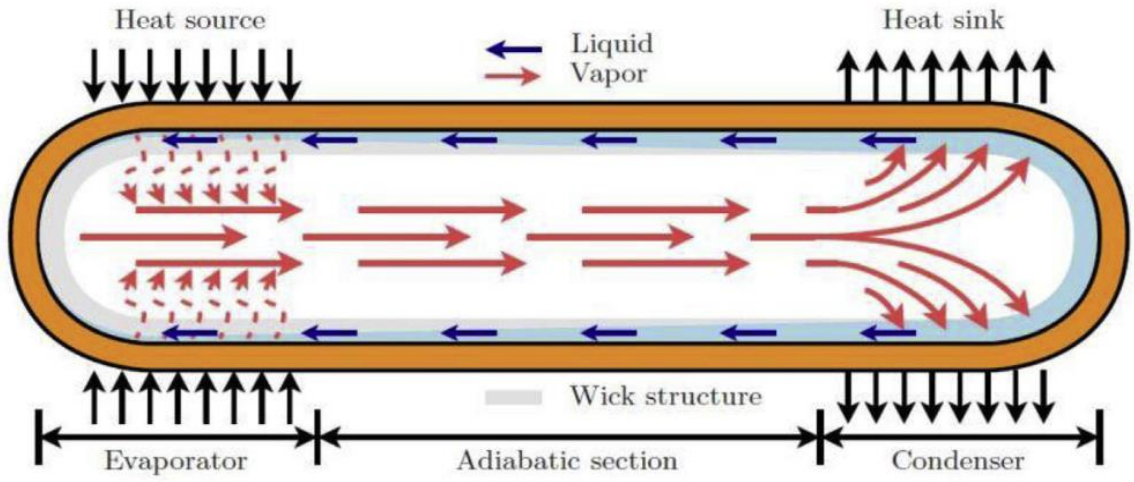

Figure 12. Schematic of conventional heat pipe tubular structure with sealed ends

As shown above n the figure heat pipe typically divided in three parts, these are the hot end (evaporating section), adiabatic part (transport section) and the cold end(condenser). In electrical vehicles the system works the liquid with in the wick absorbs excess heat from the battery cell arranged near the hot end of heat pipe and evaporates. The increase in vapor pressure and decrease in molecular density creates a pressure gradient that drives the hot vapor toward the condensing section, where it releases heat to the heat exchanger. Capillary forces within the wick then draw the condensed liquid back into the evaporator, completing the heat transfer cycle [27].

III. Jacket cooling system

Another method of cooling the battery is the jacket cooling system. In an EV battery, the jacket cooling system works by removing heat from the battery module either by direct immersion or by circulating liquid in the jacket that surrounds the battery cells. Coolant flows through the space between the jacket and the battery case and absorbs heat from the battery cells.

IV. Phase change materials (PCM)

Phase Change Material (PCM) is a direct passive solution that involves placing battery cells in a matrix of phase change materials and requires no maintenance. PCM can be used in conjunction with the other cooling methods mentioned above or as an independent solution. In electric vehicles, pcms are usually located around the battery cells or inside the battery module. As the battery cell

cools, the PCM solidifies and releases the stored heat. Pcms are low-maintenance, and this approach uses organic, inorganic, or eutectic solid-liquid phase change materials to address uneven temperature distribution throughout the battery. However, phase change materials (PCM's) have relatively low thermal conductivity which leads to slower regeneration times.as a result they are less effective in application that include fast charging followed by quick discharging and then another fast charge of the battery pack within a short period of time [27].

2.9.Studies on The EV Battery Thermal Management

Patcharin saechan et al. Investigated the air-cooled thermal management system of lithium-ion battery pack for electric vehicles. The cylindrical batteries used in the study is NCR18650B with the capacity of 3400-mah. a three-dimensional cylindrical batteries model is performing using CFD software, ANSYS fluent which is based of finite volume method. A transient thermal analysis is considered due to un steady heat generation on the battery to study the effect of inlet velocity, discharging rate and cell arrangement structure on the cooling performance. The simulated result shows that the proposed cooling system minimize the maximum the surface temperature of the battery and provides uniform temperature distribution through the battery pack [29].

M. Shahjalal *et al.* Studied on the thermal analysis of battery back for an electric motor application. Effective thermal design is developed by enclosing the battery in a high thermal conductivity material (copper and aluminum) integrated with liquid cooling system. The liquid cooling system is designed by placing the cold plate at the bottom of the battery pack. Numerical studies are carried out using COMSOL software for 72V,42Ah battery to study the effect of battery housing materials on the battery temperature. Also, they study the effect of ambient temperatures, discharge rate and coolant temperatures on the battery temperature. The result shows that 53℃ is achievable with cupper battery housing material. Additional temperature reduction is possible with the help of liquid cooling system, with 20℃ coolant temperature, the battery temperature is reduced to28℃ [6].

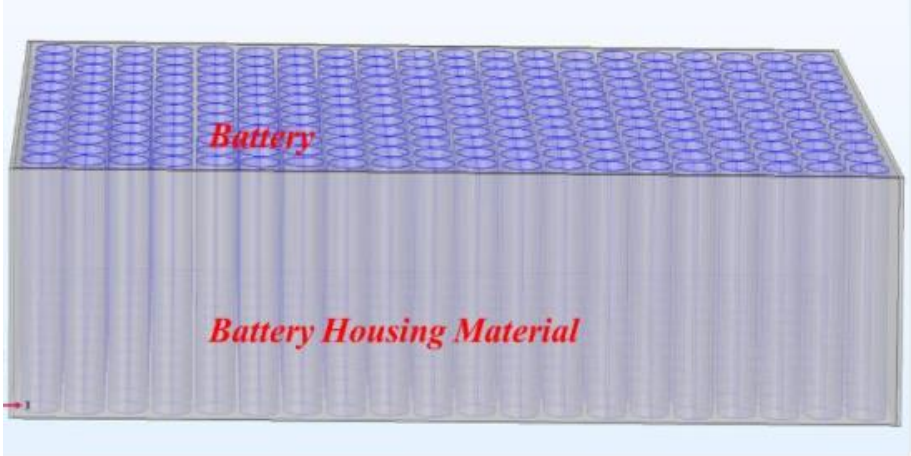

Figure 13. 43Ah electric motor battery back configuration

C. Alaoui et al. Designated and evaluated the battery thermal management system of 60Ah lithium-ion electric vehicles. They used thermo electric coolers (tecs) to manage the battery temperature when the battery is under operating conditions. The cell temperature was measured in the laboratory under different discharge rates and different ambient temperature with constant discharging current. This measurement was used to determine the heat generation rate under different ambient temperature, in order to maintain the battery operating temperatures. The result shows that, the designed battery thermal management system provides satisfactory results by decreasing the surface temperature of the cell [30].

2.10. Research Gap

According to the literature, components exposed to significant heat should effectively absorb heat from the heated component and dissipate it to the environment. Studies have also shown that even at very high air flow rates, air cooling may not sufficiently satisfy the heat dissipation requirements of the EV battery during charging and discharging processes in hot conditions. In addition, the very low thermal conductivity of air can make it difficult to cool the battery in a high temperature environment. Letin mengo (Anna 200) electric vehicle battery trays are made up of AISI 4031 steel case and the electric vehicles used free air to cooling the battery pack during charging and discharging process. This EV battery tray is subjected to heat during charging and discharging processes, which requires an investigation to enhance its thermal stability and mechanical strength.

CHAPTER THREE

MATERIALS AND METHODS

3.1. Materials For Battery Tray

Selecting the material for battery tray play a significant role in preventing thermal shocks and other external loads during charging and discharging process. Therefore, it is crucial to select the material that meets the required performance. It is preferred for battery trays to be made of lightweight materials such as aluminum, aluminum alloys and composite materials to provide the rigidity needed to support the weight of the cells. The metal case effectively withstands high temperature and pressure conditions, and because metals have high thermal conductivity, they facilitate heat management.

Table 6 materials used for battery tray in different EVs [31].

Vehicle	Material used for battery tray
BMW i3	Aluminum
Honda Fit EV	Steel
Chevrolet volt	Steel
Chevrolet spark EV	Composite
Tesla Roadster	Aluminum

3.1.1. EV Battery Tray Datasheets

The battery tray in EV is used to protect the battery cells from external crash, support cells and also used us thermal management hardware. The design of lightweight battery tray material is critical for increasing the range and efficiency of electric vehicles. There are different EVs with different battery tray structures one of those are shangan Anna 200 EVs. In Anna 200 three pack negative battery cells and three pack positive battery cells are placed separately in different compartments on the battery tray.

- EV type = shangan Anna 200
- Battery tray Material currently in use = steel AISI 4130
- Size = 1050mm*870mm*1.4mm
- Cooling system = natural air cooling
- Battery material= lithium iron phosphate
- Battery model= A10E-180
- Battery nominal capacity= 150Ah
- Nominal voltage= 115.2V
- Nominal energy = 17.28kwh
- System weight= 156Kg
- **Optimal storage temperature = -10 to 35** degrees Celsius

Figure 14. Actual picture of Letin mengo (Anna 200) electric vehicle battery pack

3.1.2. Selected Material for Anna 200 EV Battery Housing

Aluminum Metal Matrix Composites (AlMMCs) used for its good mechanical and thermal properties such as high thermal conductivity, low thermal expansion, strength, less density, excellent stiffness, lightweight, toughness, resistance to corrosion, fatigue, low creep and wear relative to non-reinforced alloy and high thermal conductivities [22].

The Al metal is selected due to its versatility and it offers ease in extrusion, good mechanical and thermal properties, formability and machinability that is generally suitable for high strength requirements and good toughness [32]. Silicon carbide is one of the commonly used structural ceramics, it has excellent mechanical properties with low density, good wear resistance, good strength and high hardness. And also has a low-cost material with a high modulus of elasticity and is used as a reinforcing phase. Compared with silicon nitride and tungsten carbide, the raw materials used to obtain silicon carbide are cheaper and the cost of the final products is low. Al-SiC is a metal matrix composite consisting of an aluminum matrix and silicon carbide as the reinforcing phase [4], [12].

AlSiC-9 material is selected for EV battery tray due to its suitability, as its coefficient of thermal expansion (CTE) aligns well with ceramic materials. AlSiC packages offers high thermal conductivity (200 W/mk) and low coefficient thermal expansion (CTE) that are compatible with electronic systems and assemblies. This compatibility helps reduce thermally induces stresses.

Table 7 properties of AlSiC composites [23].

Properties	Units	Alsic
Density	**(g/cm3)**	**3.00**
Thermal conductivity	**(W/mk)**	**200**
Coefficient of Thermal Expansion (CTE)	**(ppm/°C)**	**7.4 - 8.26**
Specific Heat Capacity	J/kg℃	**740**
Young's modulus	**Mpa**	**192**
Bend strength	**Mpa**	**450**

3.2. Numerical analysis of electric vehicle (EV) battery tray

3.2.1. Battery Tray Configuration

The battery tray in Letin mengo (Anna 200) electric vehicle is used as a thermal management hardware, protection of the battery cell from external crash and support the cells. It is located in the center of the chassis under the passenger seats to act as a semi-structural component of the vehicle and to avoid the typical deformation zones found at the front and rear.

The battery pack used in Letin mengo (Anna 200) electric vehicle consists of 360 cells in a series of parallel connection. The battery pack is usually enclosed and supported by AISI steel. However, since steel has poor thermal conductivity that causes to increase the battery tray temperature significantly. To investigate the impact of battery tray materials on temperature distribution in the battery pack AlSiC composite battery tray housing material will be studied.

Figure 15. Placement of Letin mengo (Anna 200) electric vehicle lithium-ion battery pack

4.2.2. Battery Tray Thermal Model

Lithium-ion batteries have emerged as the preferred choice for electric vehicles (EVs) due to their high efficiency, long life and specific energy. The performance of the battery is significantly affected by the operating conditions of the electric car and the surrounding environment. In extreme operating and environmental conditions, the battery generates significant heat, which can affect the rate of heat dissipation, shorten the life of the battery, and even lead to dangerous incidents such as explosions and fires (thermal leakage) [28].

The governig thermal equation describing the battery tray conduction during charge or discharge operating condition can be wriiten as follow [24], [33].

$$\boldsymbol{\rho c}\left(\frac{\partial T}{\partial t}\right) = \boldsymbol{K\partial/\partial t}\left(\frac{\partial T}{\partial y}\right) + \boldsymbol{K\partial/\partial t}\left(\frac{\partial T}{\partial y}\right) + \boldsymbol{K\partial/\partial t}\left(\frac{\partial T}{\partial z}\right) + \boldsymbol{Q}\text{.....(1)}$$

Where;

K, thermal conductivity of battery tray

Q, heat generation from the battery

Cp, specific heat capacity of material

T, battery tray temperature

P, density of material

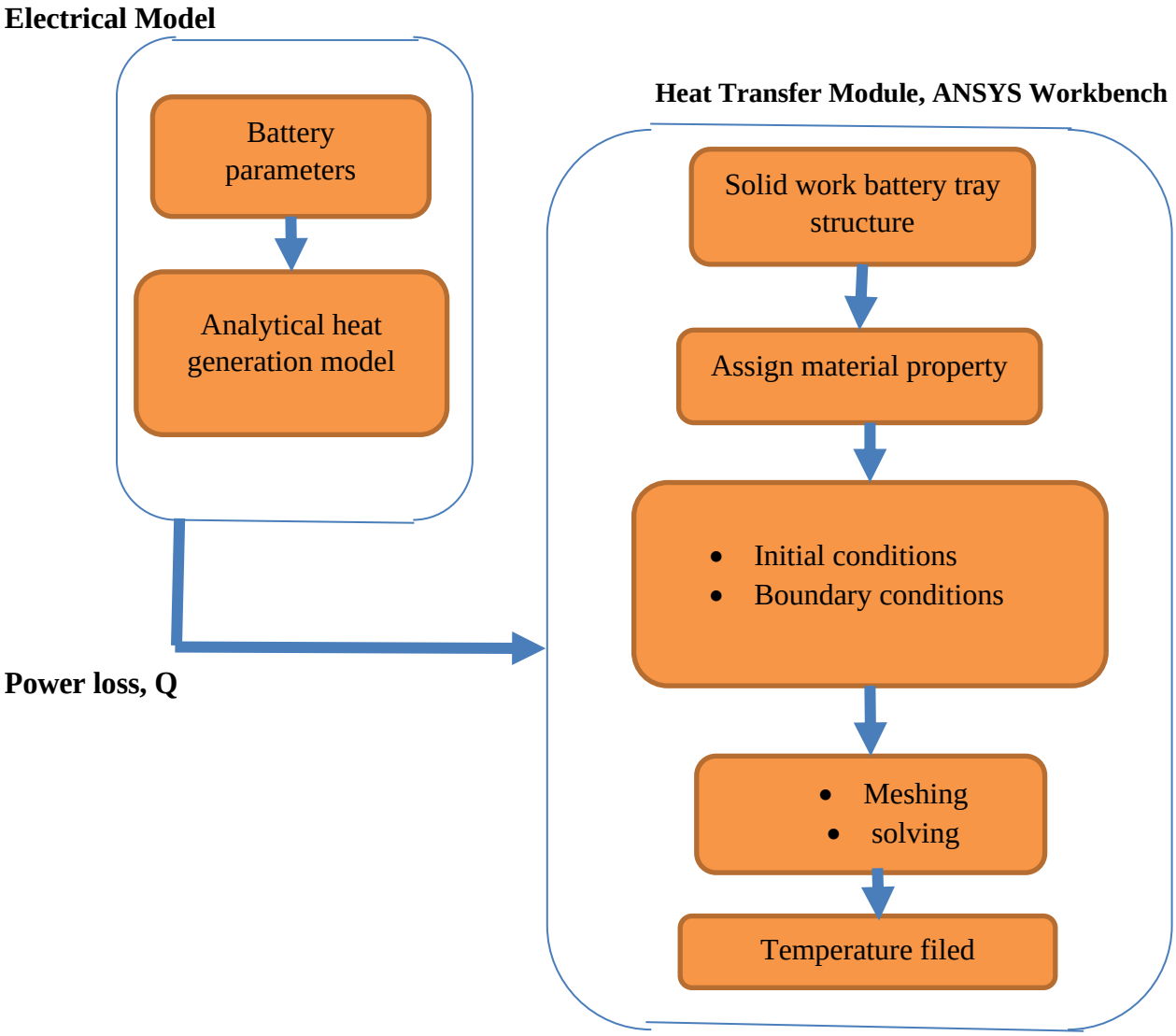

Figure 16. Thermal model setup[6].

ASSUMPTION

The following assumptions were set for the battery tray thermal model to achieve an accurate solution.

- It is assumed that the generated heat from the battery is fully transferred to the tray through conduction.
- Uniform heat generation on the battery tray surface.
- Neglect radiative heat transfer between the battery tray and the battery.
- Forced convection heat transfer is considered by applying the calculated convection heat transfer coefficient to the surface.
- The temperature of the battery tray directly affects the overall temperature of the battery because the battery tray is critical for heat dissipation. Proper temperature management is essential to ensure optimal battery performance and prevent overheating.

4.2.2.1.Heat Generation

The operating temperature of lithium-ion batteries is a key factor affecting the performance of electric vehicles. During the charging and discharging process, the temperature of the battery fluctuates due to internal heat generation, which requires the analysis of the battery's heat generation rate. This generated heat includes Joule heat and heat of reaction, which are affected by several factors, including temperature, battery aging, state of charge (SOC), and operating current.

The performance and lifespan of lithium ion battery cells are highly influnced by the thermal condition of the battery cells.therfore the thermal behavior of the battery cells is closely related to the rate of heat generationand and it is crucial to calculate heat generation under various condition.

The heat generated by the battery includes electro chemical reaction, joule heat, polarized heat and side reaction heat [34].

$$\boldsymbol{Q = Q_r + Q_j + Q_p + Q_S} \ldots\ldots\ldots\ldots (\mathbf{2})$$

Where;

Q is total heat generated by the battery cells

Q_r is the electro chemical reaction heat,which produced during the intercalation and deintercalation of lithioum ions between the anode and athode during charging and discharging.

Q_j refers joul heat, which is genetrated by internal resistance.

Q_p refers polarized heat, resulting from internal resistance due to polarizing during charging and discharging.

Q_s refers side reaction heat, This is due to the breakdown and reactivity of the electrolyte as well as thermal degradation of the separator, anode and cathode materials..

Direct measurement of the heat produced by a lithium-ion battery in an experiment is challenging due to environmental conditions and heat loss during transmission; therefore, the computational approach proposed by Bernardi et al. [35] are used. The following theoretical formula for the rate of heat generation was determined; assuming uniform heat generation in a lithium-ion battery [6], [34], [35].

$$\boldsymbol{Q_{gen} = Q_{irr} + Q_{rev}} \ldots\ldots\ldots\ldots (3)$$

$$\boldsymbol{Q = I(E - U) - IT\left(\frac{\partial E}{\partial T}\right)} \ldots\ldots\ldots\ldots\ldots (4)$$

Where;

I refer the charging and discharging current of lithium-ion battery

E refers open circuit voltage

U refers closed circuit voltage

T refers surface temperature of the battery and $\frac{\partial E}{\partial T}$ Is the temperature coefficient of open circuit voltage.

$\mathbf{Q_{irr}}$ and $\mathbf{Q_{rev}}$ represents irreversible heat and reversible heat

The first term on the right side of the equation ($\boldsymbol{I(E-U)}$) represents the irreversible reaction heat such as joule heating and electro chemical polarization which can be expressed as $\mathbf{I^2R}$, Where R is the internal resistance of lithium-ion battery. More than 70% of the generated heat is irreversible and occurs at the electrodes, electrolyte and current collector. This heat is directly affected by C-rate and is primarily defined by Joule heating in the battery cell.

During electrochemical reactions, reversible heat is generated at the cathode and anode, which is considered entropic heat, resulting from reversible entropy changes. During both charging and discharging, this heat rises as the charging rate increases from 1C to 2C before dropping to 3C.the second term ($\boldsymbol{IT\left(\frac{\partial E}{\partial T}\right)}$) represents the heat generated by reversible reaction heat and the lithium-ion battery takes a reference value of 0.042 [36]. When the values are applied to the formula the equation becomes;

$$\boldsymbol{Q = I^2R - 0.042I} \ldots\ldots\ldots\ldots\ldots (\mathbf{5})$$

And

$$\boldsymbol{I = C * N} \ldots\ldots\ldots\ldots\ldots\ldots (\mathbf{6})$$

Where;

C = battery capacity (Ah)

N = number of hours continuous discharge

The following factors affect how much heat is produced in battery cells: [38].

- During charging and discharging, the high level of current increases the temperature of the battery.
- The amount of heat removed from the battery is called depth of discharge (DOD).

- Increasing the temperature of the battery reduces the internal resistance and accelerates the electrochemical reaction.
- State of Health (SOH): the quality of the battery in relation to its optimal condition.
- Capacity availability.

According to the experiment of IFR32135-15Ah lithium-ion rechargeable cell the relationship between the equivalent internal resistance and state of charge (SOC) is modeled using polynomial functions to calculate the heat generation rate for the battery.

SOC (-)	Discharge DCR/ $m\Omega$
5%	16.2
10%	12.0
20%	9.4
30%	8.5
40%	7.8
50%	7.3
60%	7.2
70%	7.1
80%	6.8
90%	6.5
95%	6.3

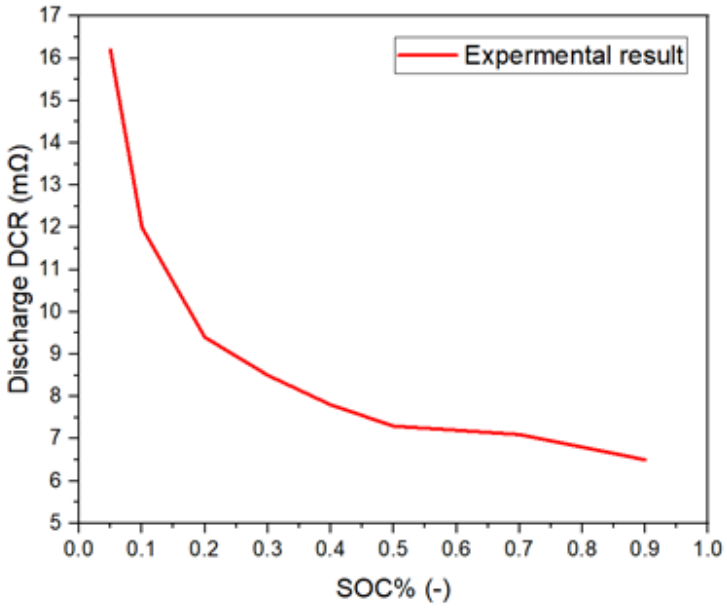

Figure 17. Experimental data for equivalent internal resistance and state of charge (SOC-) at 3C rate and 25℃ ambient temperature for IFR32135-15Ah battery cell. Via {HEFEI GUOXUAN high - tech power energy co., Ltd manufacturers}.

The results of the experimental analysis can be used to develop a battery heat generation model and to design algorithms for a battery management system. Additionally, investigating the pulse discharge characteristics of lithium batteries can offer data support for the calculation of heat sources necessary for temperature field simulations [37].

The first step to establish the thermal model is to estimate the heat generation. Due to battery loading either in discharge or charge mode, heat generation is inevitable in the battery.so,

3C SOC discharging

To get the heat generation rate in 3c first we calculate the current flows;

$$i = C * N$$

$$I = 150A * 3 = 450A$$

- **This means 150Ah EV battery can supply 450A average up to 20 minutes**

So; the heat generation in 3C is; at battery temperature 25℃

- At 5% SOC discharge

  R=16.2mΩ

  $Qgen = I^2R - 0.042\text{I}$

$$= 450 * 450 * 16.2m\Omega - 0.042(450A)$$

$$\boldsymbol{Qgen = 3262W}$$

Calculate the Surface Area: $\boldsymbol{A = 1.15m2}$

- At 5% SOC discharge the heat flux in 3C is;

Heat flux=2836W/m^2

- At 10% SOC discharge

  R=12mΩ

  $Qgen = I^2R - 0.042\text{I}$

$$= 450 * 450 * 12m\Omega - 0.042(450A)$$

$$\boldsymbol{Qgen = 2412W}$$

Calculate the Surface Area: A=1.15m^2

- At 10% SOC discharge the heat flux in 3C is; **Heat flux=2097W/m^2**

SOC	Discharge DCR/ $m\Omega$	Heat generation (W)	Heat flux(W/M^2)
5%	16.2	3262	2836
10%	12.0	2412	2097
20%	9.4	1884.6	1639
30%	8.5	1702.35	1480.3
40%	7.8	1560.6	1357
50%	7.3	1478.25	1285.43
60%	7.2	1449.1	1260.08
70%	7.1	1418.85	1233.78
80%	6.8	1377	1197.39
90%	6.5	1297.35	1128.13
95%	6.3	1256.85	1092.9

A)

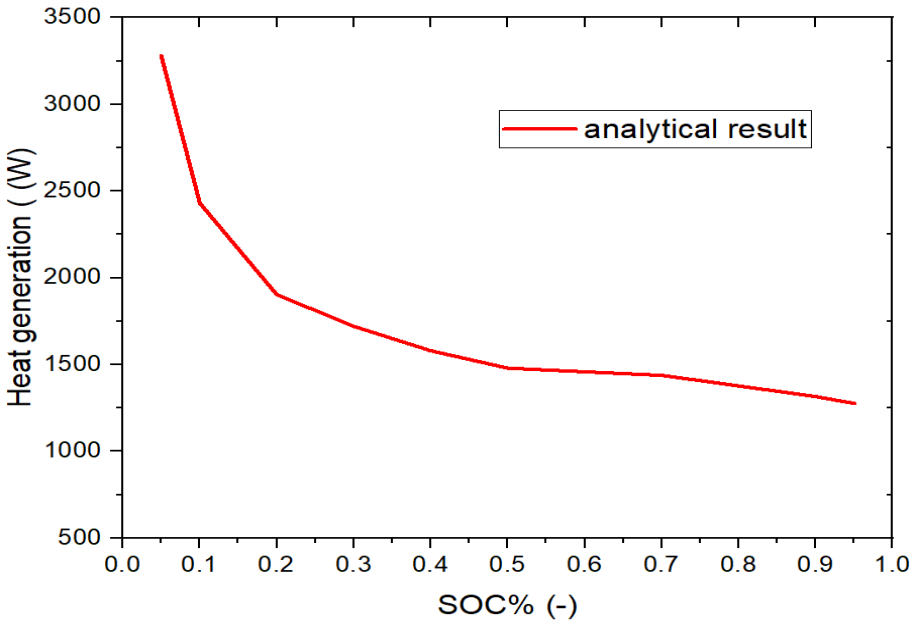

B)

Figure 18. A) table indicates 3C SOC discharging analytical values of heat flux and heat generation rate of the battery b) graph represents the relationship between heat generation and DOD at 25℃ ambient temperature.

4.2.2.2. Convective Heat Transfer Coefficient

To simulate convective behavior, convective boundary conditions are applied to all surfaces of the structure. In this model, the heat transfer coefficient by flow between the surroundings and the battery tray is determined using an empirical relationship. The average forced convection coefficient can be calculated based on the dimensionless parameters at the film temperature.

The convective heat transfer coefficient (**h**) correlation determined from the dimensionless parameters, namely the Nusselt number ($\boldsymbol{N_u}$), Prandtl ($\boldsymbol{p_r}$) and Reynolds number ($\boldsymbol{R_e}$). Different correlations are given in different conditions cited in (HOLMAN, 1986).

Convection is categorized as natural (or free) and forced convection depending on how the fluid motion is initiated. In this study, convection heat transfer is considered as forced convection.

For most engineering calculation the convection coefficient obtained from a relation as follow. (HOLMAN, 1986).

Nusselt number (Nu);

$$\boldsymbol{N_u = h.\frac{L}{K} = \frac{q_{conv}}{q_{cond}}} \ldots\ldots\ldots\ldots (\mathbf{7})$$

The Reynolds number at which the flow becomes turbulent is called the critical Reynolds number. For a flat plate, the critical Reynolds number is experimentally determined to be approximately Re critical = 5 x10^5.

Nusselt number, non-dimensional heat transfer coefficient

- The average Nusselt number for laminar flow is given by

$$\boldsymbol{N_u = 0.664 R_e^{1/2} P_r^{1/3} for\ p_r > 0.6} \ldots\ldots\ldots\ldots (\mathbf{8})$$

- The average Nusselt number for turbulent flow is given by

$$N_u = 0.037 R_e^{4/5} P_r^{1/3} for\ 0.6 < p_r < 60 \ldots\ldots\ldots\ldots (9)$$

Prandtl number, is a measure of relative thickness of the velocity and thermal boundary Layer.

$$p_r = \frac{v}{\alpha} = \mu c_p / k \ldots\ldots\ldots\ldots (10)$$

Reynolds number, ratio of inertia forces to viscous forces in the fluid

$$R_e = \frac{\rho VL}{\mu} \ldots\ldots\ldots\ldots\ldots\ldots\ldots (11)$$

Where;

R_e is Reynolds number

N_u; Nusselt number

P_r; Prandtl number

μ; thermal infusibility

v; kinematics viscosity

A; dynamic viscosity

P; density

C_p; specific heat capacity

V; velocity of the fluid

All fluid characteristics (such as density, viscosity, etc) are evaluated at film temperature (T_f);

$$T_f = (T_w + T_\infty)/2 \ldots\ldots\ldots\ldots (12)$$

The ambient temperature is 293K and the surface (wall) temperature taken the maximum optimum temperature of the system which is 308K, so from equation (9) the film temperature is

$$\boldsymbol{T_f = (T_w + T_\infty)/2}$$

$$T_f = \frac{(298 + 333)K}{2} = 315.5K$$

At T_f The value of Prandtl number ($\boldsymbol{P_r}$) = 0.707 and kinematics viscosity (**v**) =$1.559 * 10^{-5} m^2/s$ also the dynamic viscosity (μ)=1.85 *10^{-5}Kg/ms

The characteristics length of the surface ($\boldsymbol{L}$) calculated as follow,

$$\boldsymbol{L = \frac{A_s}{P}} \ldots\ldots\ldots\ldots (\mathbf{13})$$

A is area of the surface and P is perimeter of the surface.

- The heat transfer coefficient on the battery tray surface heated from the bottom can be calculated as follows. From equation (13) and (11),

$$L_H = \frac{A_H}{P_H} = \frac{0.85m^2}{24m} = 0.035m$$

From equation (8) and (10) the value of Reynolds number and Nusselt number is

$$\boldsymbol{R_e = \frac{\rho VL}{\mu}} = 8111.48$$

Hence the flow is laminar flow we use equation (8) to find Nusselt number

$$N_u = \mathbf{0.664} \boldsymbol{R_e}^{\mathbf{1/2}} \boldsymbol{P_r}^{\mathbf{1/3}}$$

$$N_u = 54$$

From equation (6) $h = N_u . \frac{K}{L} = \mathbf{41} \frac{\boldsymbol{W}}{\boldsymbol{M^2}} . \boldsymbol{K}$

Improved efficiency y $= (\boldsymbol{Q_{initial} - Q_{final}})/\boldsymbol{Q_{initial}}$ **…….. (14)**

4.2.3. FEA Modeling and Analysis Method

The battery tray studied in this paper is taken from Letin mengo (Anna 200) electric vehicle as shown below in figure 19.the chosen battery tray consists 360 cylindrical lithium-ion phosphate batteries with a related specification of nominal capacity 150Ah and 115.2V Nominal voltage. The EV drawn power from 115.2V battery packs. To achieve 115.2V Nominal voltage cells are connected in series and 36 strings (each strings contain 10 cells) with a current rating of 150A are connected in parallel.

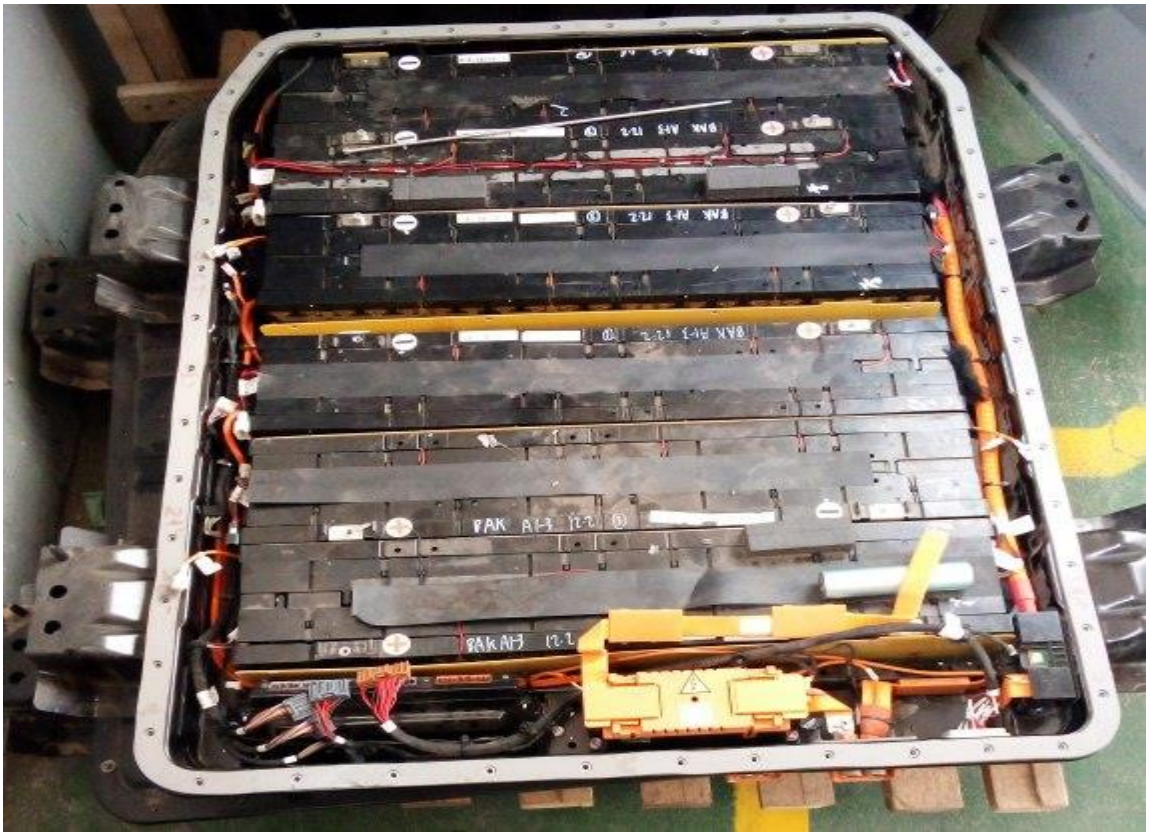

Figure 19. typical configuration of 150Ah Letin mengo (Anna 200) electric vehicle battery pack

The cell used in this simulation is taken from commercial cells (IFR32135-15Ah battery cell, China,) with different internal resistance based on its discharging rate. The specification of the batteries used in the battery pack are listed in the following table;

Table 8 specification of 15Ah battery (for single battery)

Specification of Battery	Value
Diameter	33.6mm
Hight	136.3
Weight	268g
Model name	IFR32135-15Ah
Product type	Lithium-ion phosphate rechargeable
Standard capacity	15Ah
Nominal voltage	3.2V
Optimum working temperature	-30℃ to 60℃

4.2.4. Thermal Modelling of Battery Tray on ANSYS Workbench

A three-dimension model of battery tray is performed using commercial ANSYS workbench software. A transient simulation model is considered due to the un steady heat generation of the battery. The procedure to modeling the battery tray in ANSYS workbench is as follow.

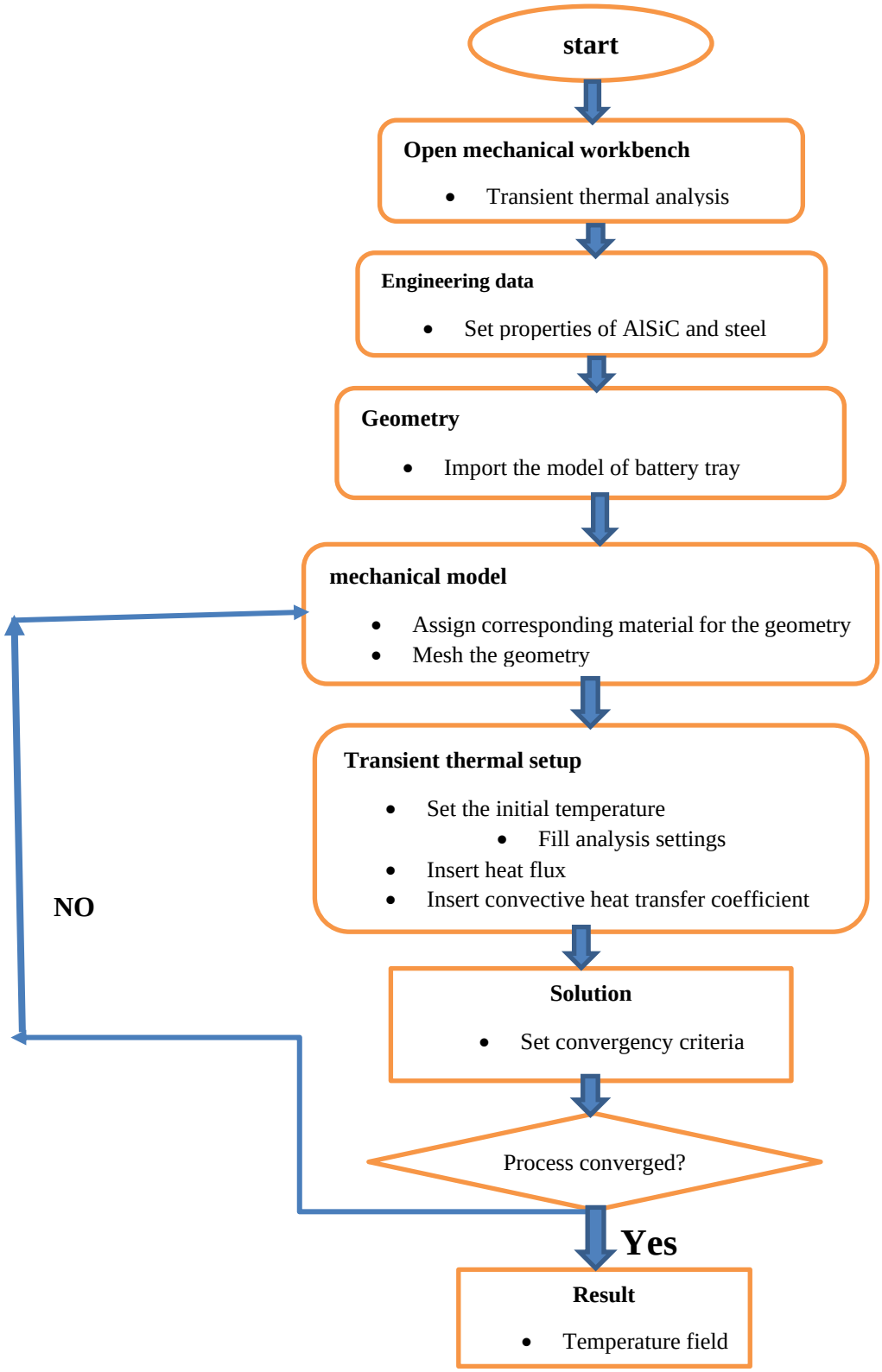

Figure 20. Steps used on mechanical workbench

4.2.4.1.ANSYS Transient Thermal Setup

The ANSYS transient thermal setup is used to simulate a model involving nonlinear temperature boundary condition analysis makes use of the set up to calculate the temperature based on specified initial condition, boundary condition and material property at discrete nodes created through the software's discretization process. Like other finite element method (FEM) transient thermal analysis follows three primary steps for solving problems; pre-processing, analysis and post processing.

Engineering data

ANSYS consists engineering data that used to select an appropriate material with its physical properties. The material used for the battery tray plays a crucial role in thermal management of the battery pack, when the battery cells are arranged in a dense, compact configuration.[6]

A 3D thermal model based on finite element analysis is developed to determine transient temperature of the battery tray and to investigate the use of AlSiC composite materials for reducing temperature. Steel 4130 and AlSiC material properties are used for this simulation.in the thermal analysis of battery tray, there are three critical material properties; density, specific heat and thermal conductivity. The following table represents properties of steel4130 and AlSiC material used in the simulation.

Table 9 thermo physical properties of steel4130 and AlSiC materials used in the simulation

Material properties	4130 steels	AlSiC composite	Units
Density	7850	3000	$kg/m3$
Thermal conductivities	42.5	200	$W/m℃$
Specific heat	477	740	$J/kg℃$

Import The Geometry

From the geometry section select the import geometry from the menu that having a file type of 'IGS' since the geometry was developed using SOLIDWORK SOFTWARE.

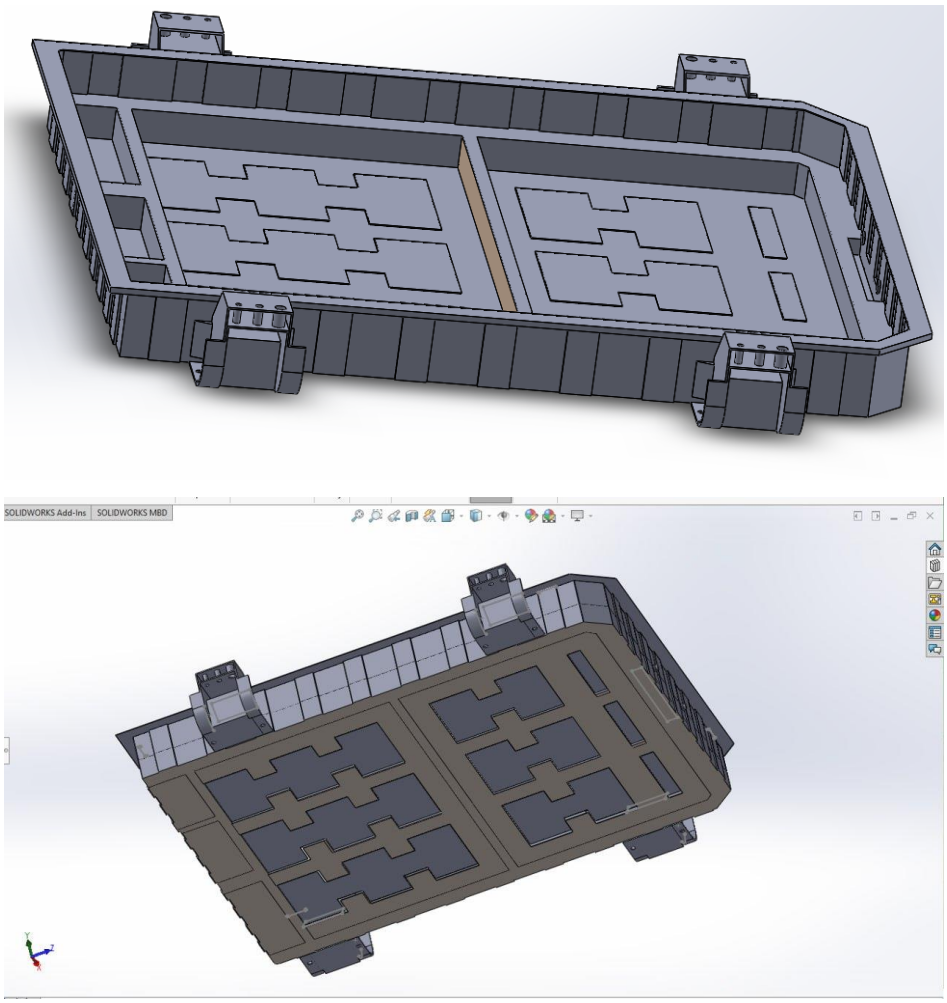

Figure 21. 3D solid work modeling of Letin mengo (Anna 200) electric vehicle battery tray

Model

In this section of transient thermal setup, the parameters that control the simulations (model, transient thermal and solution) are selected. The model section contains geometry, coordinate system, mesh and connections. In the geometry section proper materials are assigned based on the provided engineering data. Set local and global coordinate system and in the connection section,

contact regions between the battery tray and handling. After this meshing is performed using suitable techniques for the problem and named selections assigned here. The transient thermal setup includes initial temperature, analysis setting and boundary conditions are defined. In the solution section, the output values are specified.

Mesh

It is discretizing a complex object in to smaller a well-defined element in order to simulate the physical behavior easily. The size of the elements is selected after the grid independence tests are performed. This study used a triangular mesh due to its irregular structure. This type of mesh is suitable for varies irregular surface and topology.

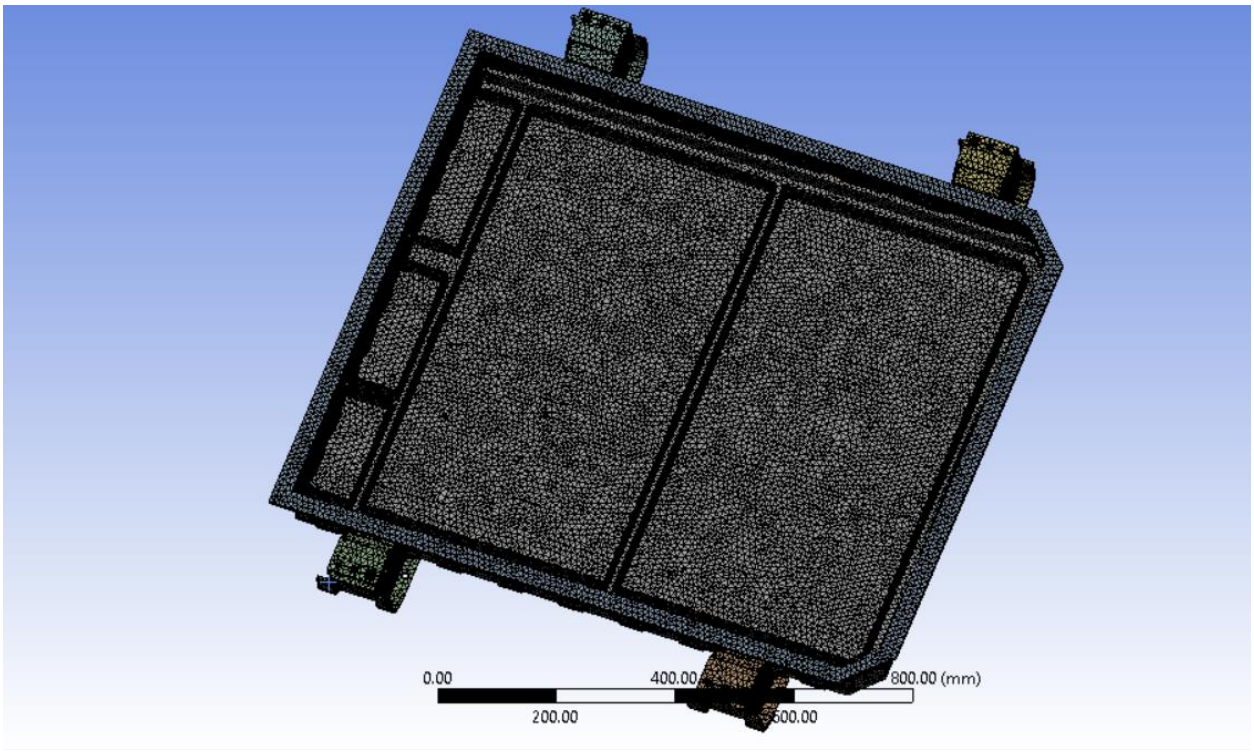

Figure 22 meshed model of the studied EV battery tray

Transient Thermal Analysis

The transient thermal setup includes initial temperature, analysis setting and boundary conditions. The ambient temperature of the battery tray set to in ambient temperature of 25℃,to simulate the surface temperature of the battery.in the boundary condition the calculated analytical value of the heat flux discharging (5%,10%,20%,30%,40%,50%,60%,70%,80%,90%,95%) are assigned. And also, convective heat transfer coefficient(h) is assigned as calculated.

In the analysis setting; minimum time step, maximum time step and end of time steps are assigned. In the study the minimum and the maximum time step number used in the simulation are 0.1 and 0.001 also the end of time steps is 30 second.

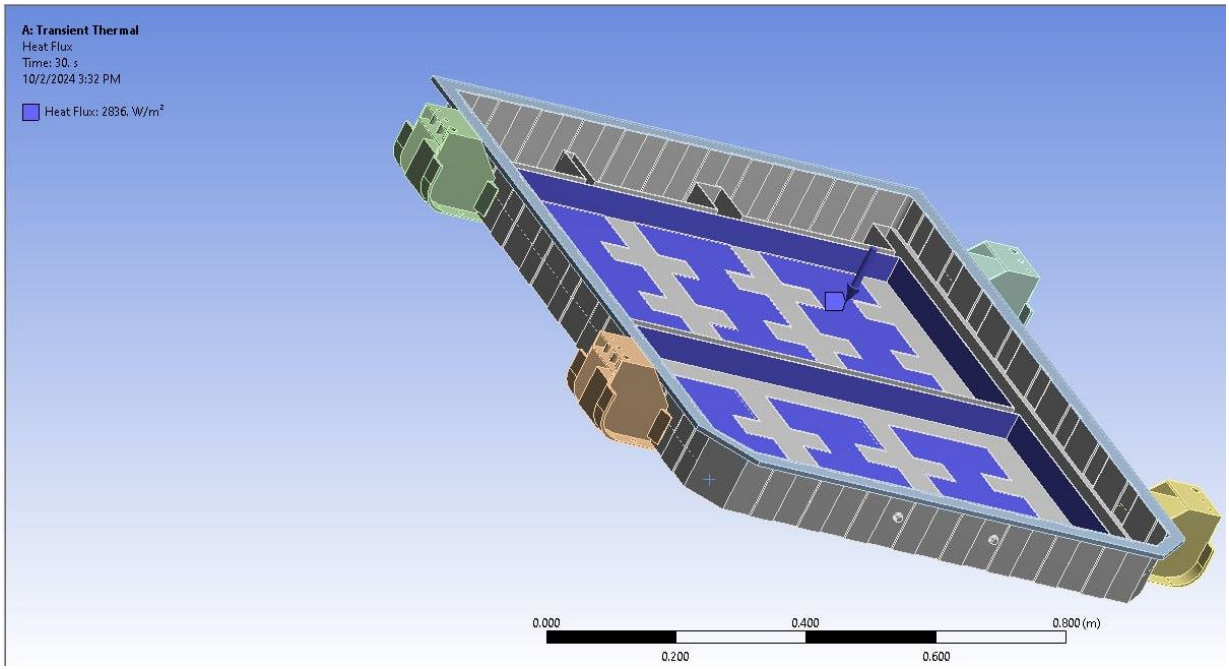

Figure 23. Applied heat flux on the battery tray surface at 5% SOC discharge and 25℃ ambient temperature.

Solution

In this phase of the simulation setup, the model is run to obtain a solution. The maximum and minimum temperature plots over discharging rate are displayed in the solution information section. Additionally, the solution information also shows the convergence of the solution at each time step of the analysis.

4.2.4.2.Mesh Convergence Test

The size of the mesh is an important factor in solving numerical solution as it greatly affect the reliability and accuracy of the calculations. In these cases, the same SOC discharge (3C) condition is applied and the ambient temperature of the battery tray is set to 25 ◦C. After all of these parameters were considered and applied, the total number of mesh nodes and elements were discovered to be 598387 and 383182, respectively.

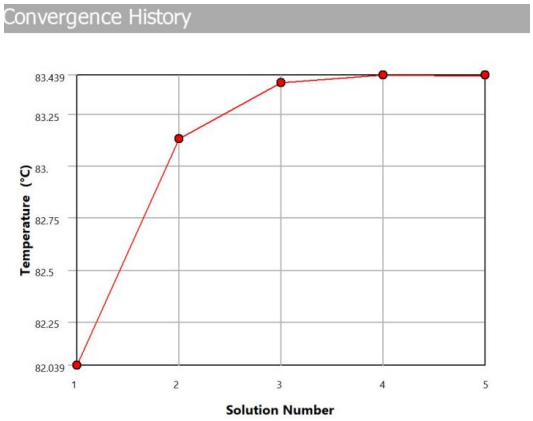

	Temperature (°C)	Change (%)	Nodes	Elements
1	82.039		70937	35330
2	83.134	1.3253	154712	85671
3	83.402	0.32225	281746	170004
4	83.439	4.4768e-002	598387	383182
5	83.439	7.3149e-005	896900	593449

Figure 24. Mesh convergence test

CHAPTER 4

RESULT AND DISCUSSION

The operating temperature of the battery is crucial for its safety, lifespan, and performance and proper thermal management of lithium-ion batteries is essentially important in hot climate.[29] in these studies, two factors such as battery tray material and cooling systems are analyzed in order to control the battery tray temperature. This section explains the result obtained from the battery tray under different SOC discharging and different battery tray materials with cooling system.

4.1. Simulation of Surface Temperature of Battery Tray in Natural State

In this analysis simulation of thermal behavior of battery tray made from two different materials are performed. The current 150Ah Letin mengo (Anna 200) EV battery tray material (steel4130) and aluminum silicon carbide metal matrix composite (alsic MMC) materials are used for the simulation. In the natural working state of the battery pack, the heat dissipates from the battery without the aid of any active cooling mechanism. The goal of this analysis is to understand the impact of battery tray materials on the surface temperature distributions.

During discharging process, heat is generated from the battery due to the internal resistance, electrochemical reaction and other factors. For the natural working state of the battery pack, the heat generated from the (Anna 200) EV battery is provided in the above figure 18.

4.1.1. Simulation with steel 4130 materials

For the first simulation; The thermal behavior of the battery tray when enclosed with steel 4130 is analyzed. The simulation is setup with steel4130 material under 5% SOC discharging (95% depth of discharge) and the ambient temperature is considered 25℃.

From equation (4) we can get the following calculated heat flux values and using those heat flux value at different SOC discharging and convective heat transfer coefficient of $h = (41\frac{W}{M^2}.K)$. Using those boundary conditions, we can determine the effect of depth of discharge in the battery tray surface temperature.

The resulting temperature distribution of the battery tray is presented as shown below in figure (24). It is observed that the operating temperature rise significantly, reaching up to 83. 47℃.this temperature exceeds the operating optimum working temperature of the lithium-ion battery which is typically less than 60℃. This increase in temperature is due to the low thermal conductivity of the steel materials and making it an unsuitable material for battery tray to dissipate heat effectively.

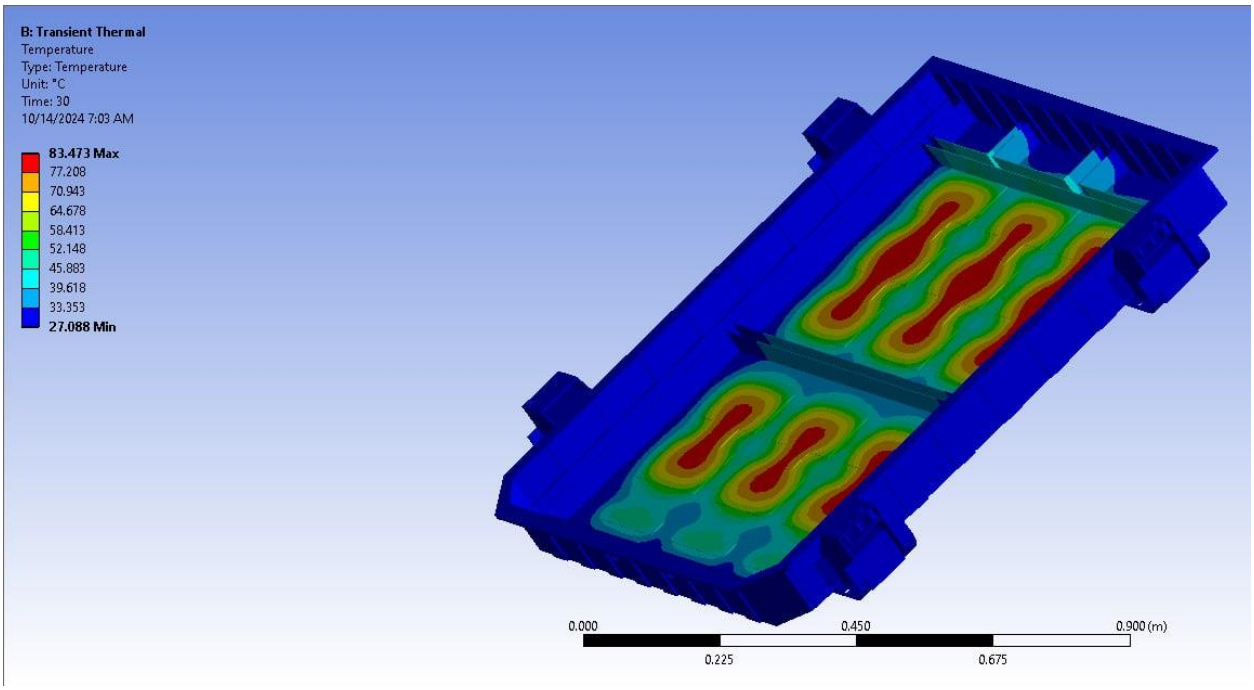

Figure 25. Temperature contour of the entire battery tray in steel4130 material at 3C discharge and 25℃ ambient temperature.

Steel gives excellent strength, excellent fatigue resistance, it is simple to create a complex shape and assemblies (easy to fabrication) and making it suitable for structural applications. However, it has low corrosion resistance, heavy weight, low thermal conductivities (TC) and high coefficient of thermal expansion (CTE) values that may result in thermally induced stresses that can cause the device to fail by cracking. This induces the overheating of the internal components, thermal stress and leads to reduce the overall efficiency of the battery's and also the life time of the battery. It is preferred that the battery trays are fabricated from lightweight materials like aluminum, aluminum

alloy and composite materials which ensures thermal stability and the rigidity required to support the weight of the cells [31].

To reduce the temperature of the battery tray, materials with light weight, good mechanical strength, high thermal conductivity (TC) and low coefficient of thermal expansion (CTE) such as aluminum silicon carbide metal matrix composite (alsic MMC) are selected.

4.1.2. Simulation with alsic MMC materials

To improve the thermal performance of the battery tray, alsic MMC materials with high thermal conductivity (TC) and low coefficient of thermal expansion (CTE) are used for the second simulation.

The simulation is setup with alsic material under 5% SOC discharging (95% depth of discharge) and the ambient temperature is considered 25℃. Figure (22) shows that the maximum temperature raises of the battery tray at 3C 5% SOC discharging rate and an ambient temperature of 25℃. The result shows that the maximum operating temperature of the battery tray surface is reduced to 69.6℃ due to the high thermal conductivity material of alsic MMC.

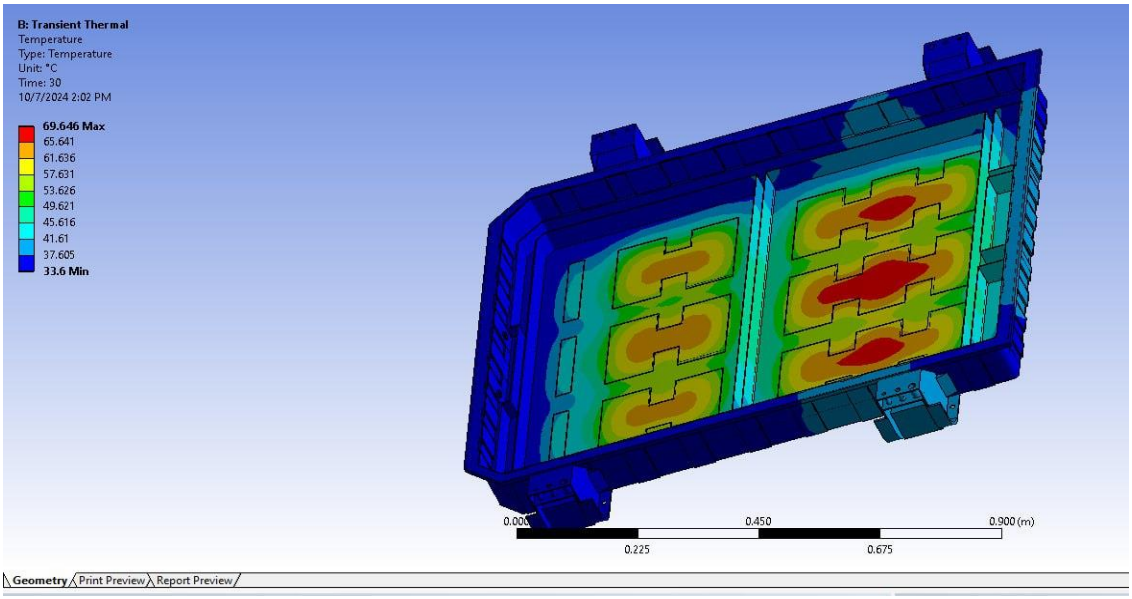

Figure 26. Temperature contour of the entire battery tray in alsic MMC material at 3C discharge and 25℃ ambient temperature.

In this result using aluminum silicon carbide metal matrix composite (alsic MMC) we can reduce the battery tray surface temperature from **83.47**℃ (with steel4130) to **69.9**℃**.**however, this is still not sufficient to bring the battery discharge temperatures in to the safe range between **(-30**℃ **to 60**℃**).** Therefore, an additional cooling method is needs to keep the battery temperature with in safe limits under 3C discharging rate conditions.to achieve this an effective cooling system should be configured at the bottom of the battery back.

4.2. Effect of Different SOC Discharging in (3C-Rate)

To predict the impact of battery temperature variation on EV battery tray performance, heat generation during discharging process must be analyzed. This largely depend on the operating conditions such as environmental temperature and state of charge (SOC) [38].

In below the table (10) at the same (25℃) ambient temperature, the heat generation rate increases at the higher depth of discharge (DOD) or the lower SOC discharge.

Table 10. Analytical calculated heat flux value at different SOC discharge and at 25℃ ambient temperature.

SOC (-)	Heat flux***(W/M^2)***
5%	2836
10%	2097
20%	1639
30%	1480.3
40%	1357
50%	1285.43
60%	1260.08
70%	1233.78
80%	1197.39
90%	1128.13
95%	1092.9

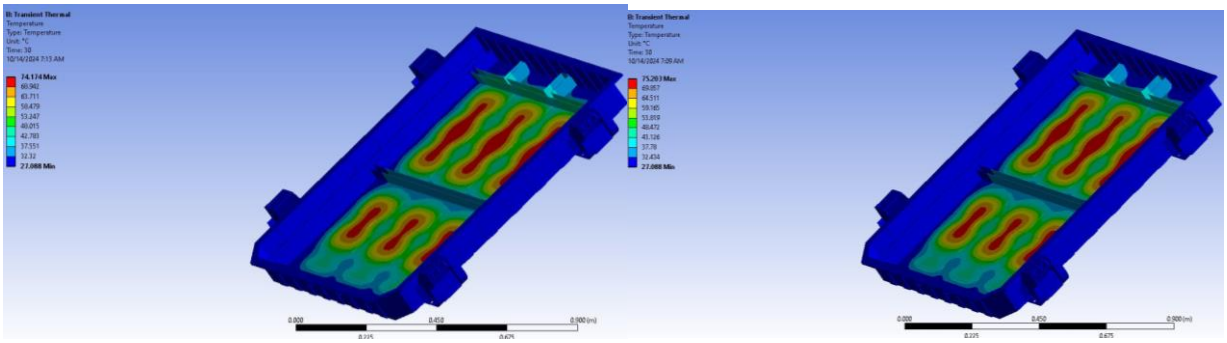

A)

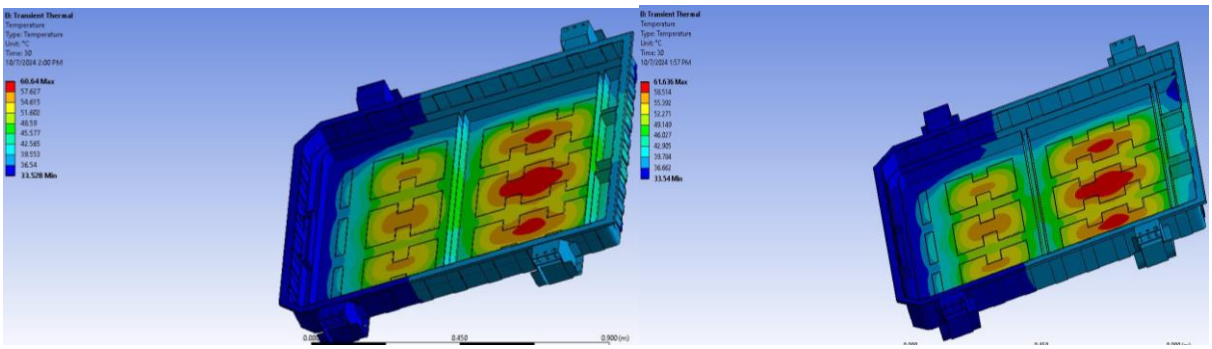

B)

Figure 27. A) surface temperature distribution of EV battery tray under 95%and 50% SOC discharging a) using steel4130 b) using alsic MMC materials

The resulting temperature distribution of the battery tray is presented as shown below in figure (23). It is observed that in the early stage of discharging processes the battery tray surface temperature is lower. In the last stage of discharging, the temperature of the battery tray is increasing due to the battery direct resistance (DC) increases under the large SOC conditions, leading to an increase in irreversible joule heat. This indicates that the operating surface temperature of the battery tray rises significantly under the lower SOC discharge (higher DOD). This indicates that at higher depth of discharge under 3C discharging rate the battery temperature must be maintained and controlled by using different battery cooling thermal management system.

Table 11. Surface temperature of battery tray under different SOC discharging

SOC (-) discharge	**Steel4130 material,** Surface temperature of the battery tray (℃)	**Alsic MMC**, Surface temperature of the battery tray (℃)
5%	83.47	69.64
10%	79.53	65.8
20%	77.09	63.46
30%	76.24	62.64
40%	75.58	62.008
50%	75.2	61.63
60%	75.07	61.5
70%	74.92	61.36
80%	74.73	61.18
90%	74.36	60.82
95%	74.17	60.64

When the battery terminal voltage decreases as the depth of discharge (DOD) increases. When the DOD exceeds 90% (=10% SOC discharging), the terminal voltage drops rapidly and the irreversible joule heat is proportional to the rate at which the terminal voltage decreases and the discharge rate.as a result more heat is generated in the battery during higher depth of discharge (during low SOC discharging). The high heat generation at low SOC discharging leads to increasing the surface temperature of the battery tray [38].

efficiency $=(Q_{initial} - Q_{final})/Q_{initial}$

$$Q_{initial} = h * A * (83 - Tamb)$$

$$Q_{initial} = 15628.81W$$

$$Q_{final} = h * A * (69.9 - Tamb)$$

$Q_{final} = 14976.726$ Efficiency = 0.0417

4.3. Numerical Analysis of Cooling System Impact on Battery Thermal Management

Managing the temperature of the battery is crucial to avoid degradation and thermal runaway. Hence the battery is generating heat during charging and discharging processes. For this case an effective thermal management is essential to maintained a safe operating temperature. Ensuring thermal safety improves EV reliability and reduce the risk of battery pack failure and for such type of purpose liquid cooled thermal management provides excellent cooling performance [6].

A numerical case study has been conducted to predict the impact of liquid coolant on the battery tray's temperature distribution. The ANSYS fluent set up is used to simulate the surface temperature distribution of battery trays using an adequate liquid cooling system.

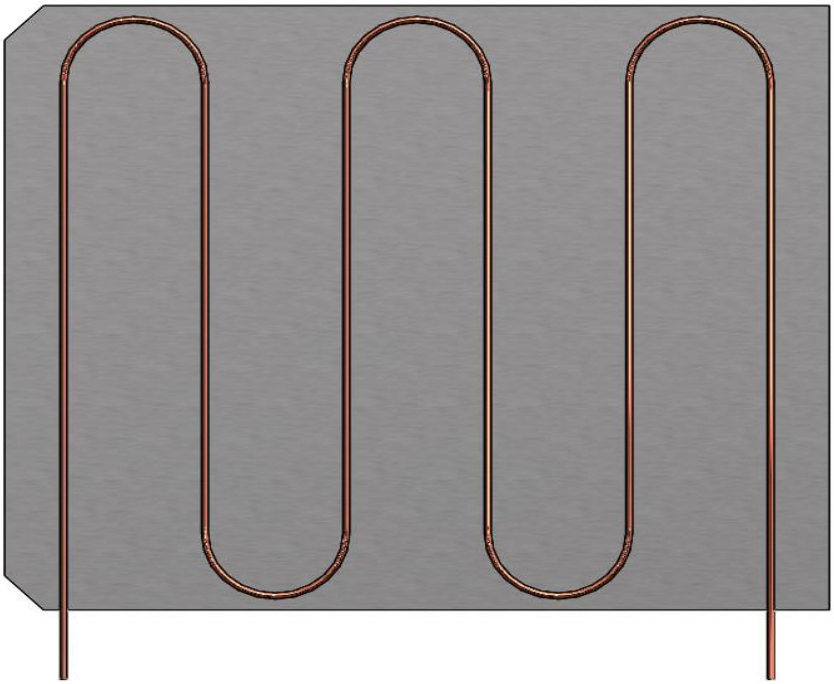

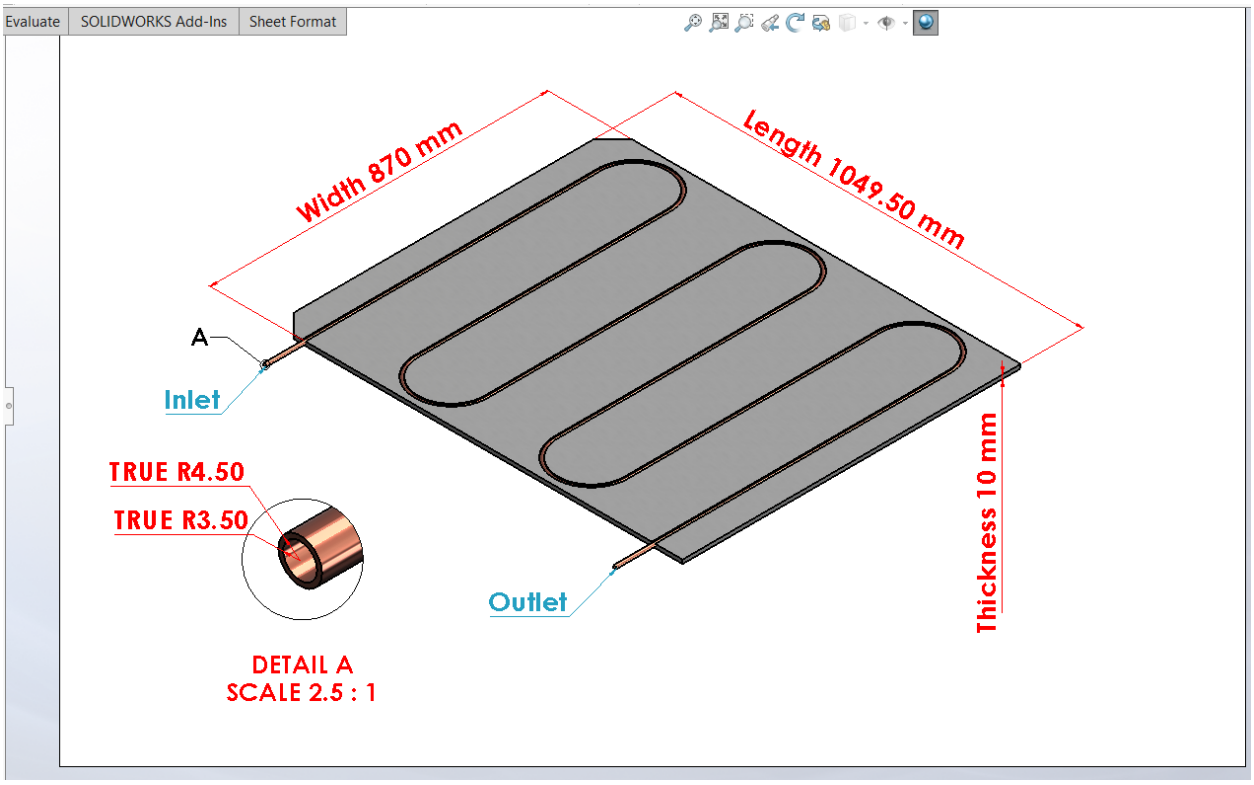

Figure 28. Liquid cold plate for Letin mengo (Anna 200) electric vehicles battery pack

Table 12. Specification of the liquid cold plate

Parameters	Value
Liquid cold plate size	1000mm*870mm*10mm
Outer diameter of the channel	9mm
Inner diameter of the channel	7mm
Channel	Cu
Coolant working temperature	20℃

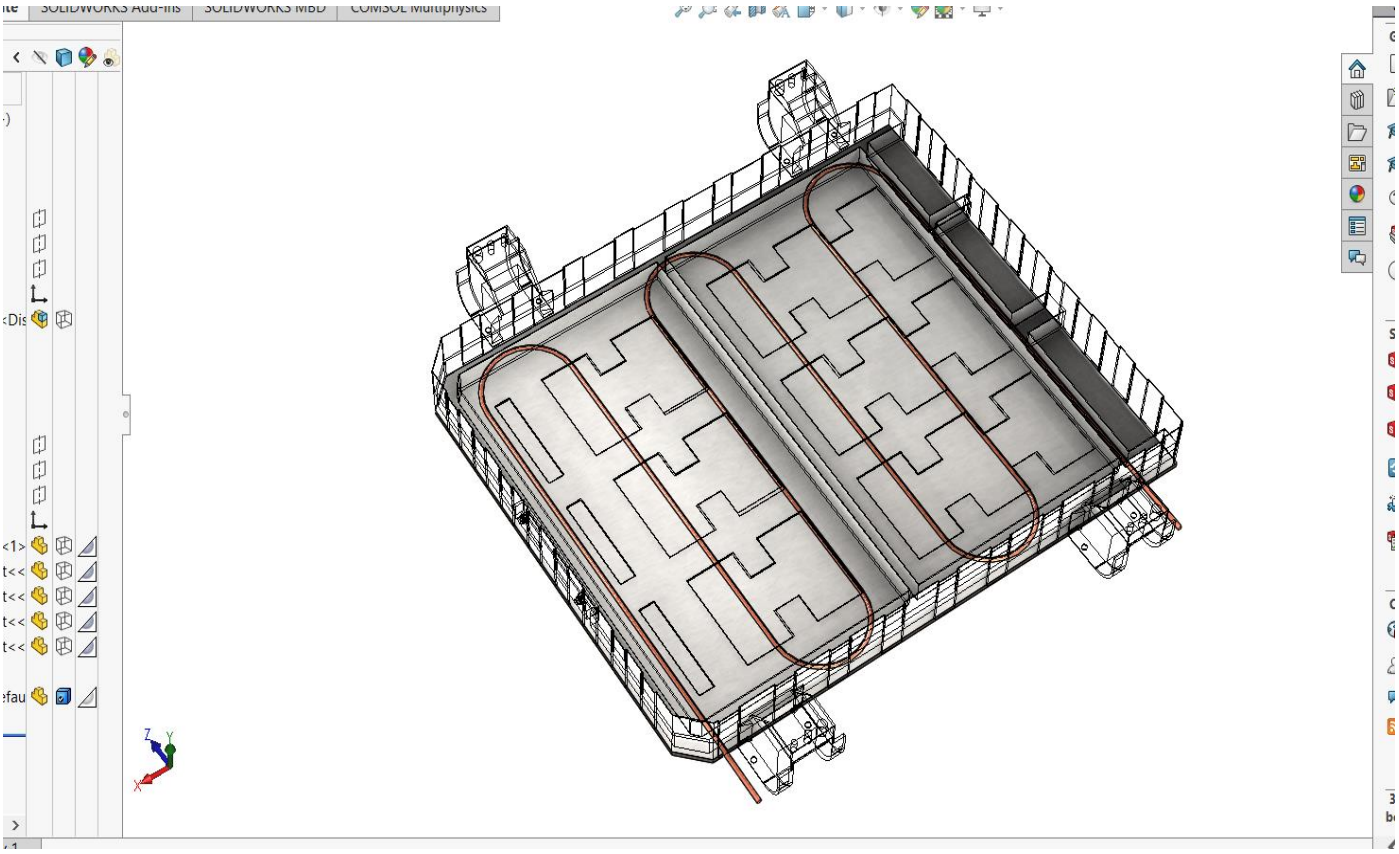

Figure 29. EV battery tray with cold plate

In this study, the coolant temperature is set to 20 °C. A fixed heat flux boundary condition is applied at the bottom of the battery tray along with a power loss corresponding to the 3C discharge rate.

In the previous result, the battery tray operating temperature can reach up to 69.9℃ at 25℃ ambient temperature and under 5% SOC discharge (95% depth of discharge).to keep the battery tary temperature additional simulation is performed to analyze the impact of liquid cooling system.

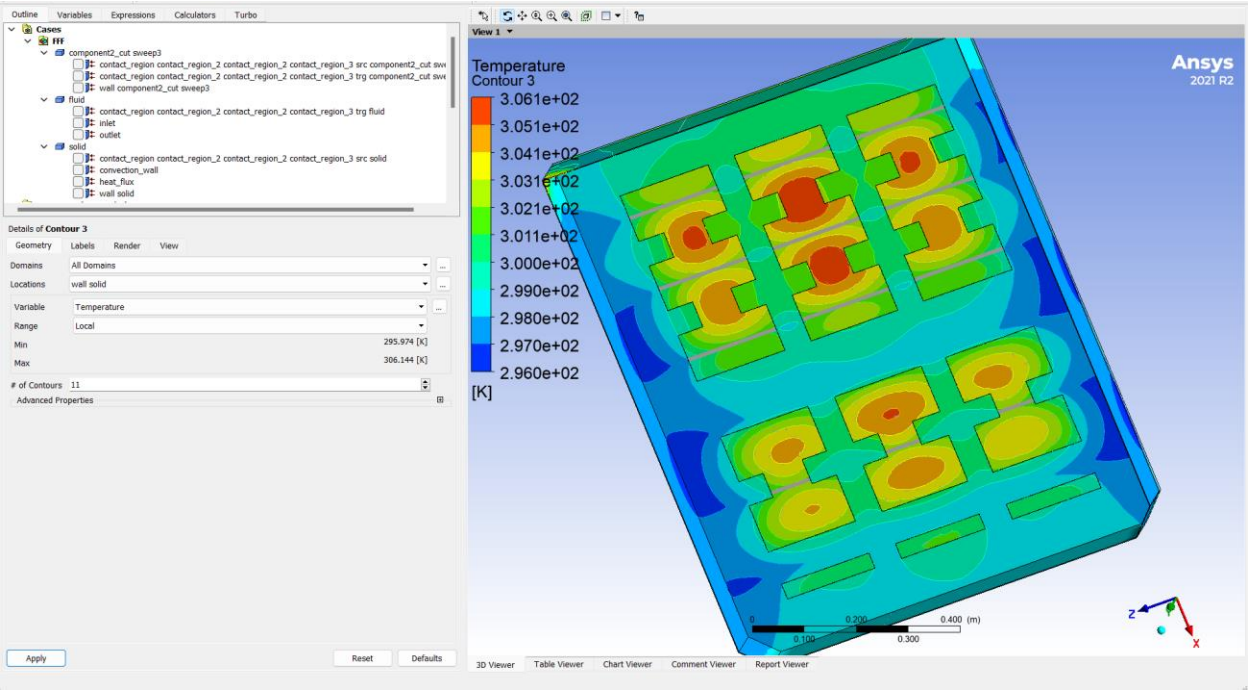

A)

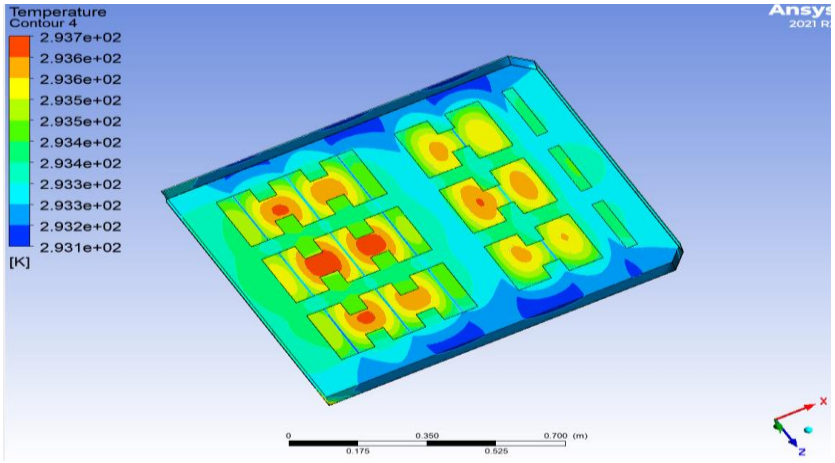

B)

Figure 30. Temperature contours of the battery tray in alsic housing with cold plate a) under 5% SOC and b) under 95% SOC discharging.

Table 13. Battery tray surface temperature simulation result under maximum and minimum heat generation on the battery tray using liquid cooling system.

SOC discharging	Maximum surface temperature (℃)	Temperature of coolant (℃)
5%	33.1	20
95%	20.7	20

The use of liquid cooling effectively reduces the high temperature levels. The figure (30) above the result shows that under 3C rate 5% SOC discharging condition, the battery temperature rises to 33.1℃ . It observed that the addition of liquid cooling system has a significant impact on the reduction of battery tray temperatures. The temperature under high depth of discharge (DOD) reduces the surface temperature from 69.9℃to 33. 1℃. The cold plate helps to reduce the battery tray operating temperature to an acceptable limit. The result suggest that a battery tray made from high thermal conductivity material is necessary for battery temperature management and additionally external liquid cooled thermal management needs to be employed when the battery is operating at higher discharging rate like 3C.

A cold plate which has internal tube for circulating a coolant is integrated directly to the bottom surface of the battery trays for liquid coolant to carry the heat from the hot component. The cold plate absorbs heat directly from the battery pack and providing efficient cooling through the system. Cold plates are mostly preferred in electric vehicles (EV's)because of the strict space limitation.[27]

4.4. Impact simulation of EV Battery Tray

4.4.1. Deformation

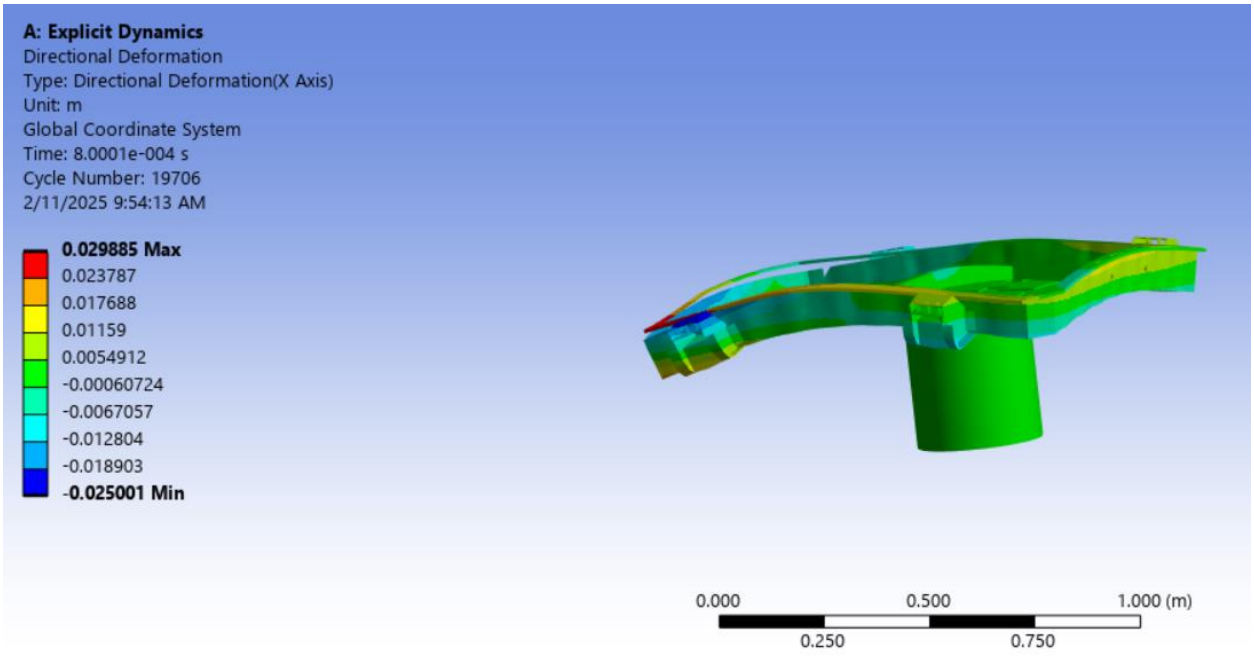

a)

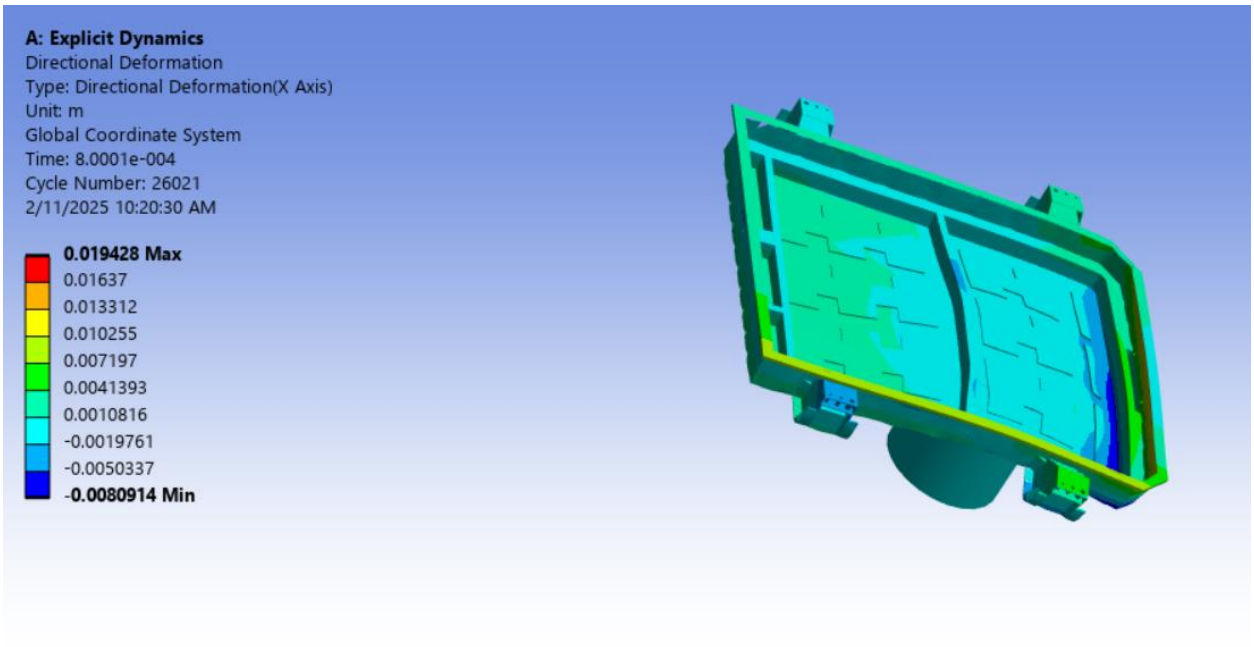

b)

Figure 31. directional deformation of a) steel4130 materials and b) Aluminum silicon carbide composite (AlSiC) material EV battery Tray.

Table 13 maximum deformation of different material EV battery Tray

materials	Maximum deformation
steel4130	0.029885m
AlSiC	0.019428m

the analysis is performed using the ANSYS workbench software and the result shows that Aluminum silicon carbide composite material of electric vehicle battery tray experiences significantly less deformation compared to conventional steel4130 materials.

4.4.2. Equivalent(von-misses) stress

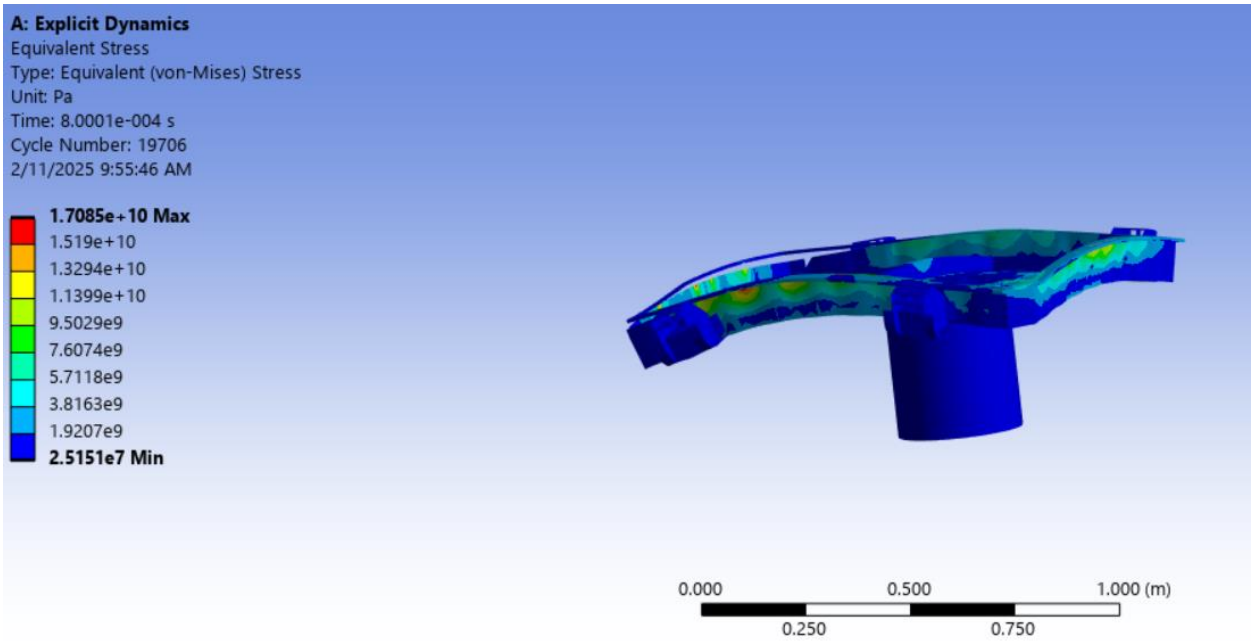

a)

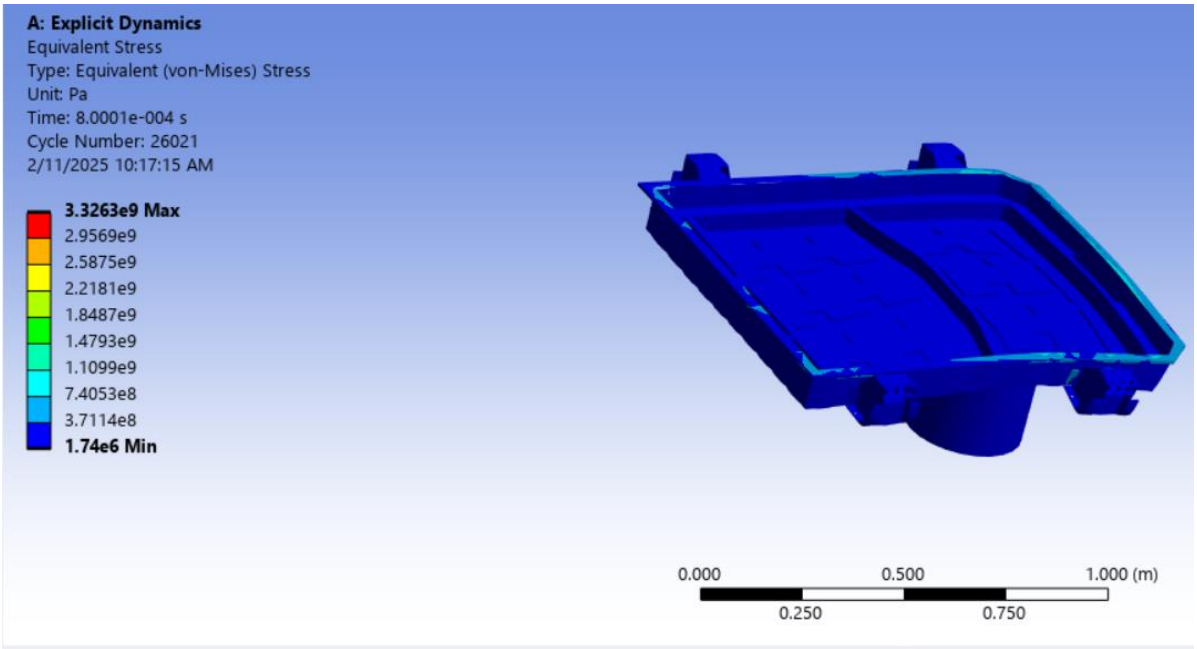

b)

Figure 32. equivalent (von misses) stress of a) steel4130 materials and b) Aluminum silicon carbide composite (AlSiC) material EV battery Tray.

The analysis shows that the Aluminum silicon carbide composite (AlSiC) material Letin mengo (Anna 200) electric vehicles battery tray experiences the lowest equivalent (von-misses) voltage compared to the conventional steel tray under the same impactors. This suggests that the EV battery tray is exposed to less stress, has a lighter weight and offers excellent performance.

CHAPTER FIVE

CONCLUSION AND RECOMMENDATION

5.1. Conclusion

This study presents a numerical simulation that provides an effective cooling solution for Letin mengo (Anna 200) electric vehicles battery tray during operating process. The cooling solution combines high thermal conductivity battery housing material with liquid cooling systems. The numerical evaluation indicates that using high TC Aluminum silicon carbide metal matrix composite material battery tray can reduce the surface temperatures from 83.47℃ steel4130 material housing to 69.64℃ at 3C discharging rate and it increases the efficiency by 4.17%. Further temperature reductions are achievable with liquid cooling (cold plate). The cooling system also reduce the battery temperature from 69.64℃ to 33.1 ℃with a coolant temperature of 20℃. This analysis show that this cooling system can maintain safe battery temperature up to a 3C discharge rate. Therefore, the system offers an enhanced safety by maintain the battery with in optimal temperature range during operating process. in the explicit dynamic analysis, the deformation and equivalent (von misses) stress of AlSiC EV battery tray is less than the convectional steel4130 EV battery tray. so, the AlSiC MMC EV battery tray is exposed to less stress, has a lighter weight and offers excellent performance.

5.2. Recommendation

The study provides valuable insights into effective thermal management strategies for EV battery trays, with potential to contribute to more efficient and safer electric vehicles in the future. While the cooling system proved effective, further research is needed to assess alternative cooling techniques or hybrid approaches that integrate advanced materials with superior thermal and mechanical properties. Additionally, a detailed analysis needed in different environmental temperature is recommended for future research to evaluate the influence of this thermal management solutions on the EV battery tray.

REFERENCES

[1] J. Lindgren and P. D. Lund, "Effect of extreme temperatures on battery charging and performance of electric vehicles," *Journal of Power Sources*, vol. 328, pp. 37–45, Oct. 2016, doi: 10.1016/j.jpowsour.2016.07.038.

[2] Z. Rao, S. Wang, M. Wu, Z. Lin, and F. Li, "Experimental investigation on thermal management of electric vehicle battery with heat pipe," *Energy Conversion and Management*, vol. 65, pp. 92–97, Jan. 2013, doi: 10.1016/j.enconman.2012.08.014.

[3] C. Linse and R. Kuhn, "Design of high-voltage battery packs for electric vehicles," in *Advances in Battery Technologies for Electric Vehicles*, Elsevier, 2015, pp. 245–263. doi: 10.1016/B978-1-78242-377-5.00010-8.

[4] M. Z. Bukhari, D. Brabazon, and M. S. J. Hashmi, "Application of Metal Matrix Composite of CuSiC and AlSiC as Electronics Packaging Materials".

[5] S. S. Sidhu, S. Kumar, and A. Batish, "Metal Matrix Composites for Thermal Management: A Review," *Critical Reviews in Solid State and Materials Sciences*, vol. 41, no. 2, pp. 132–157, Mar. 2016, doi: 10.1080/10408436.2015.1076717.

[6] M. Shahjalal *et al.*, "A Numerical Thermal Analysis of a Battery Pack in an Electric Motorbike Application," *Designs*, vol. 6, no. 4, p. 60, Jun. 2022, doi: 10.3390/designs6040060.

[7] I. D. Ibrahim, T. Jamiru, R. E. Sadiku, W. K. Kupolati, S. C. Agwuncha, and G. Ekundayo, "The use of polypropylene in bamboo fibre composites and their mechanical properties – A review," *Journal of Reinforced Plastics and Composites*, vol. 34, no. 16, pp. 1347–1356, Aug. 2015, doi: 10.1177/0731684415591302.

[8] F. Nturanabo, L. Masu, and J. Baptist Kirabira, "Novel Applications of Aluminium Metal Matrix Composites," in *Aluminium Alloys and Composites*, K. Omar Cooke, Ed., IntechOpen, 2020. doi: 10.5772/intechopen.86225.

[9] A. Kumar Sharma, R. Bhandari, A. Aherwar, R. Rimašauskienė, and C. Pinca-Bretotean, "A study of advancement in application opportunities of aluminum metal matrix composites," *Materials Today: Proceedings*, vol. 26, pp. 2419–2424, 2020, doi: 10.1016/j.matpr.2020.02.516.

[10] K. Karvanis, D. Fasnakis, A. Maropoulos, and S. Papanikolaou, "Production and mechanical properties of Al-SiC metal matrix composites," *IOP Conf. Ser.: Mater. Sci. Eng.*, vol. 161, p. 012070, Nov. 2016, doi: 10.1088/1757-899X/161/1/012070.

[11] X. He, X. Qu, S. Ren, and C. Jia, "Net-shape forming of composite packages with high thermal conductivity," *Sci. China Ser. E-Technol. Sci.*, vol. 52, no. 1, pp. 238–242, Jan. 2009, doi: 10.1007/s11431-008-0346-8.

[12] B. Siddharthan, R. Rajiev, S. Saravanan, and T. K. Naveen, “Effect of Silicon Carbide in Mechanical Properties of Aluminium Alloy Based Metal Matrix Composites,” *IOP Conf. Ser.: Mater. Sci. Eng.*, vol. 764, no. 1, p. 012040, Feb. 2020, doi: 10.1088/1757-899X/764/1/012040.

[13] C. A. J. Miranda, R. M. P. Libardi, S. Marcelino, and Z. M. Boari, “AVERAGE THERMAL STRESS IN THE Al+SiC COMPOSITE DUE TO ITS MANUFACTURING PROCESS,” 2013.

[14] Md. H. Rahman and H. M. M. A. Rashed, “Characterization of Silicon Carbide Reinforced Aluminum Matrix Composites,” *Procedia Engineering*, vol. 90, pp. 103–109, 2014, doi: 10.1016/j.proeng.2014.11.821.

[15] V. Mohanavel, K. Rajan, S. S. Kumar, S. Udishkumar, and C. Jayasekar, “Effect of silicon carbide reinforcement on mechanical and physical properties of aluminum matrix composites,” *Materials Today: Proceedings*, vol. 5, no. 1, pp. 2938–2944, 2018, doi: 10.1016/j.matpr.2018.01.089.

[16] K. Zemani *et al.*, “Numerical analysis of an experimental ballistic test of Al/SiC functionally graded materials,” *Composite Structures*, p. 117909, Jan. 2024, doi: 10.1016/j.compstruct.2024.117909.

[17] K. A. R. Kumar, K. Balamurugan, S. A. Vendan, and J. B. Raj, “Investigations on thermal properties, stress and deformation of Al/SiC metal matrix composite based on finite element method,” *Sci. Tech.*, 2014.

[18] P. Van Trinh, J. Lee, P. N. Minh, D. D. Phuong, and S. H. Hong, “Effect of oxidation of SiC particles on mechanical properties and wear behavior of SiCp/Al6061 composites,” *Journal of Alloys and Compounds*, vol. 769, pp. 282–292, Nov. 2018, doi: 10.1016/j.jallcom.2018.07.355.

[19] R. Zare, H. Sharifi, M. R. Saeri, and M. Tayebi, “Investigating the effect of SiC particles on the physical and thermal properties of Al6061/SiCp composite,” *Journal of Alloys and Compounds*, vol. 801, pp. 520–528, Sep. 2019, doi: 10.1016/j.jallcom.2019.05.317.

[20] S. Sarapure, B. P. Shivakumar, and M. B. Hanamantraygouda, “Investigation of Corrosion Behavior of SiC-Reinforced Al 6061/SiC Metal Matrix Composites Using Taguchi Technique,” *J Bio Tribo Corros*, vol. 6, no. 2, p. 31, Jun. 2020, doi: 10.1007/s40735-020-0328-3.

[21] T. H. Nam, G. Requena, and H. P. Degischer, “Modelling and Numerical Computation of Thermal Expansion of Aluminium Matrix Composite with Densely Packed SiC Particles”.

[22] A. K. Sharma, R. Bhandari, and C. Pinca-Bretotean, “Impact of silicon carbide reinforcement on characteristics of aluminium metal matrix composite,” *J. Phys.: Conf. Ser.*, vol. 1781, no. 1, p. 012031, Feb. 2021, doi: 10.1088/1742-6596/1781/1/012031.

[23] M. A. Occhionero and R. W. Adams, "AlSiC, and AlSiC Hybrid Composites for Flip Chips, Optoelectronics, Power, and High Brightness LED Thermal Management Solutions," in *2005 6th International Conference on Electronic Packaging Technology*, Shenzhen, China: IEEE, 2005, pp. 1–5. doi: 10.1109/ICEPT.2005.1564720.

[24] Z. Ye and X. Fu, "Experimental and simulation investigation on suppressing thermal runaway in battery pack," *Sci Rep*, vol. 14, no. 1, p. 12723, Jun. 2024, doi: 10.1038/s41598-024-62408-1.

[25] V. G. Choudhari, D. A. S. Dhoble, and T. M. Sathe, "A review on effect of heat generation and various thermal management systems for lithium ion battery used for electric vehicle," *Journal of Energy Storage*, vol. 32, p. 101729, Dec. 2020, doi: 10.1016/j.est.2020.101729.

[26] J. Vetter *et al.*, "Ageing mechanisms in lithium-ion batteries," *Journal of Power Sources*, vol. 147, no. 1–2, pp. 269–281, Sep. 2005, doi: 10.1016/j.jpowsour.2005.01.006.

[27] S. Arora, "Selection of thermal management system for modular battery packs of electric vehicles: A review of existing and emerging technologies," *Journal of Power Sources*, vol. 400, pp. 621–640, Oct. 2018, doi: 10.1016/j.jpowsour.2018.08.020.

[28] A. G. Olabi *et al.*, "Battery thermal management systems: Recent progress and challenges," *International Journal of Thermofluids*, vol. 15, p. 100171, Aug. 2022, doi: 10.1016/j.ijft.2022.100171.

[29] P. Saechan and I. Dhuchakallaya, "Numerical study on the air-cooled thermal management of Lithium-ion battery pack for electrical vehicles," *Energy Reports*, vol. 8, pp. 1264–1270, Apr. 2022, doi: 10.1016/j.egyr.2021.11.089.

[30] C. Alaoui, "Solid-State Thermal Management for Lithium-Ion EV Batteries," *IEEE Trans. Veh. Technol.*, vol. 62, no. 1, pp. 98–107, Jan. 2013, doi: 10.1109/TVT.2012.2214246.

[31] S. Arora, W. Shen, and A. Kapoor, "Review of mechanical design and strategic placement technique of a robust battery pack for electric vehicles," *Renewable and Sustainable Energy Reviews*, vol. 60, pp. 1319–1331, Jul. 2016, doi: 10.1016/j.rser.2016.03.013.

[32] P. Mukhopadhyay, "Alloy Designation, Processing, and Use of AA6XXX Series Aluminium Alloys," *ISRN Metallurgy*, vol. 2012, pp. 1–15, Apr. 2012, doi: 10.5402/2012/165082.

[33] N. Yang, X. Zhang, G. Li, and D. Hua, "Assessment of the forced air-cooling performance for cylindrical lithium-ion battery packs: A comparative analysis between aligned and staggered cell arrangements," *Applied Thermal Engineering*, vol. 80, pp. 55–65, Apr. 2015, doi: 10.1016/j.applthermaleng.2015.01.049.

[34] C. Zhang *et al.*, "A Li-Ion Battery Thermal Management System Combining a Heat Pipe and Thermoelectric Cooler," *Energies*, vol. 13, no. 4, p. 841, Feb. 2020, doi: 10.3390/en13040841.

[35] C.-W. Zhang, S.-R. Chen, H.-B. Gao, K.-J. Xu, Z. Xia, and S.-T. Li, "Study of Thermal Management System Using Composite Phase Change Materials and Thermoelectric Cooling Sheet for Power Battery Pack," *Energies*, vol. 12, no. 10, p. 1937, May 2019, doi: 10.3390/en12101937.

[36] C.-W. Zhang, S.-R. Chen, H.-B. Gao, K.-J. Xu, Z. Xia, and S.-T. Li, "Study of Thermal Management System Using Composite Phase Change Materials and Thermoelectric Cooling Sheet for Power Battery Pack," *Energies*, vol. 12, no. 10, p. 1937, May 2019, doi: 10.3390/en12101937.

[37] B. Jin, Q. Fei, S. Wang, Y. Wang, and W. Zou, "Experimental Study on Pulse Discharge Characteristics of Square Power Lithium-Ion Battery," in *Advances in Transdisciplinary Engineering*, M. Chen, M. Giorgetti, Z. Li, Z. Chen, B. Jin, and R. K. Agarwal, Eds., IOS Press, 2022. doi: 10.3233/ATDE220520.

[38] Y. Xie, S. Shi, J. Tang, H. Wu, and J. Yu, "Experimental and analytical study on heat generation characteristics of a lithium-ion power battery," *International Journal of Heat and Mass Transfer*, vol. 122, pp. 884–894, Jul. 2018, doi: 10.1016/j.ijheatmasstransfer.2018.02.038.

APPENDIX

Appendix A

Data sheets

Table A1; experimental results of internal resistance at different temperature and soc discharge

A.5 不同温度&不同 SOC 的放电 DCR Discharge DCR at Different Temperature and SOC

3C 30s 放电 Discharge DCR/mΩ								
T/SOC	-30℃	-20℃	-10℃	0℃	10℃	25℃	45℃	55℃
5%	/	/	/	/	/	16.2	10.2	9.0
10%	/	/	/	/	29.1	12.0	7.0	6.1
20%	/	/	/	23.9	17.1	9.4	5.9	5.4
30%	/	58.9	31.1	19.5	13.6	8.5	5.7	5.1
40%	/	53.3	26.6	17.1	12.0	7.8	5.3	4.9
50%	98.0	48.1	23.8	15.8	11.1	7.3	5.0	4.5
60%	91.7	44.3	22.1	15.0	10.5	7.2	4.7	4.2
70%	86.1	41.7	21.1	14.6	10.4	7.1	4.9	4.4
80%	82.0	40.0	20.5	14.3	10.1	6.8	4.6	4.2
90%	78.4	38.6	19.9	14.0	9.8	6.5	4.3	3.8
95%	76.8	38.1	19.7	13.8	9.6	6.3	4.1	3.7

Table A2; thermophysical properties of dry air

Dry Air - Thermodynamic and Physical Properties

Temperature (K) (deg C)	Specific Heat - c_p - (kJ/kgK)	Specific Heat - c_v - (kJ/kgK)	Ratio of Specific Heats - k - (c_p/c_v)	Dynamic Viscosity - μ - (10^{-5} kg/m s)	Thermal Conductivity (10^{-5} kW/m K)	Prandtl Number	Kinematic Viscosity 1) - ν - (10^{-5} m^2/s)	Density 1) - ρ - (kg/m^3)	Thermal Diffusivity - α - (10^{-6} m^2/s)
175	1.0023	0.7152	1.401	1.182	1.593	0.744	0.586	2.017	
200	1.0025	0.7154	1.401	1.329	1.809	0.736	0.753	1.765	10.23
225	1.0027	0.7156	1.401	1.467	2.020	0.728	0.935	1.569	
250	1.0031	0.7160	1.401	1.599	2.227	0.720	1.132	1.412	15.72
275	1.0038	0.7167	1.401	1.725	2.428	0.713	1.343	1.284	
300	1.0049	0.7178	1.400	1.846	2.624	0.707	1.568	1.177	22.18
325	1.0063	0.7192	1.400	1.962	2.816	0.701	1.807	1.086	
350	1.0082	0.7211	1.398	2.075	3.003	0.697	2.056	1.009	29.50
375	1.0106	0.7235	1.397	2.181	3.186	0.692	2.317	0.9413	
400	1.0135	0.7264	1.395	2.286	3.365	0.688	2.591	0.8824	37.66
450	1.0206	0.7335	1.391	2.485	3.710	0.684	3.168	0.7844	
500	1.0295	0.7424	1.387	2.670	4.041	0.680	3.782	0.7060	
550	1.0398	0.7527	1.381	2.849	4.357	0.680	4.439	0.6418	
600	1.0511	0.7640	1.376	3.017	4.661	0.680	5.128	0.5883	
650	1.0629	0.7758	1.370	3.178	4.954	0.682	5.853	0.5430	
700	1.0750	0.7879	1.364	3.332	5.236	0.684	6.607	0.5043	
750	1.0870	0.7999	1.359	3.482	5.509	0.687	7.399	0.4706	

Appendix B

B1; ANSYS transient thermal analysis simulation result

1) Surface temperature of battery tray at 10% SOC discharging under steel4130 and alsic battery tray materials.

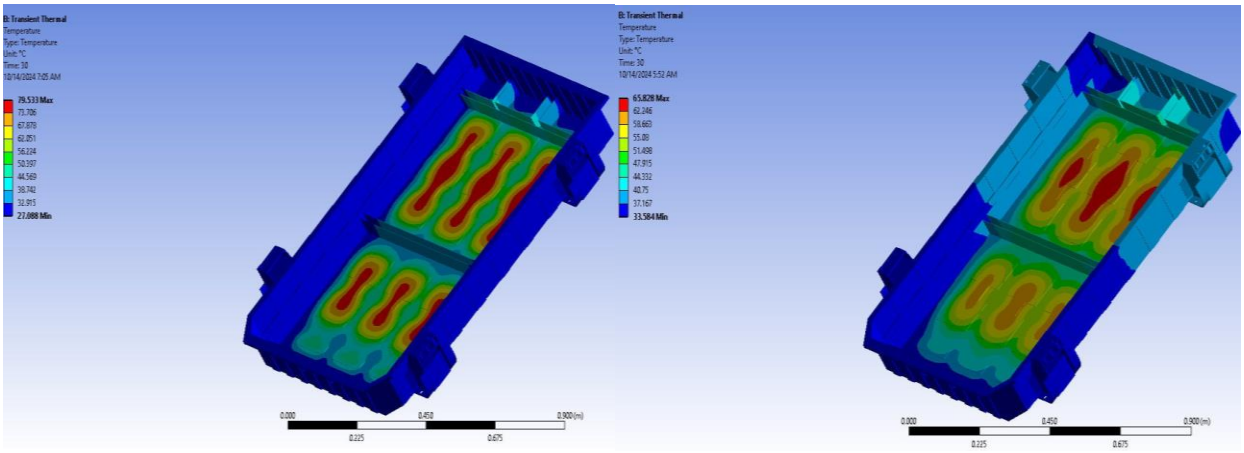

2) Surface temperature of battery tray at 20% SOC discharging under steel4130 and alsic battery tray materials.

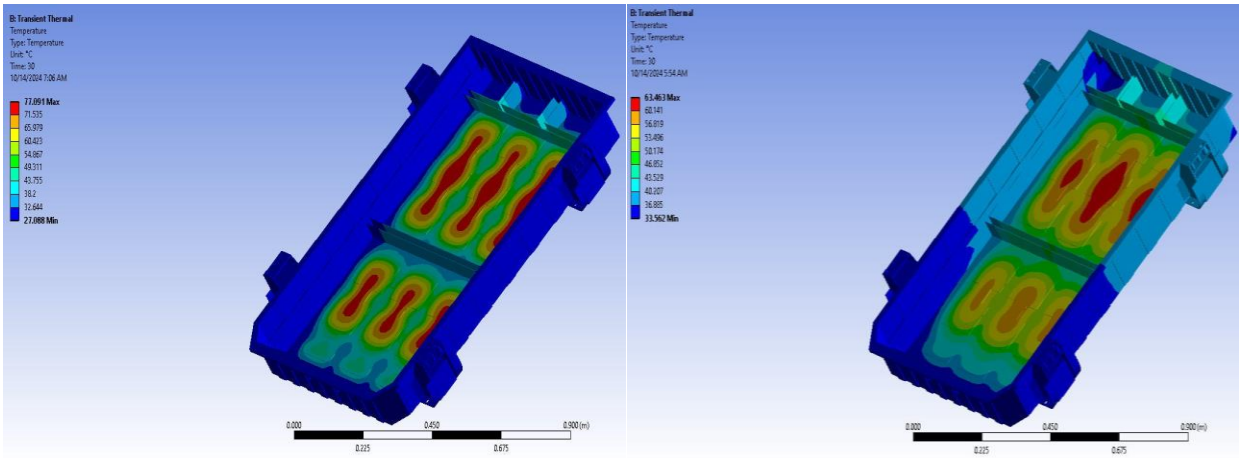

3) Surface temperature of battery tray at 30% SOC discharging under steel4130 and alsic battery tray materials.

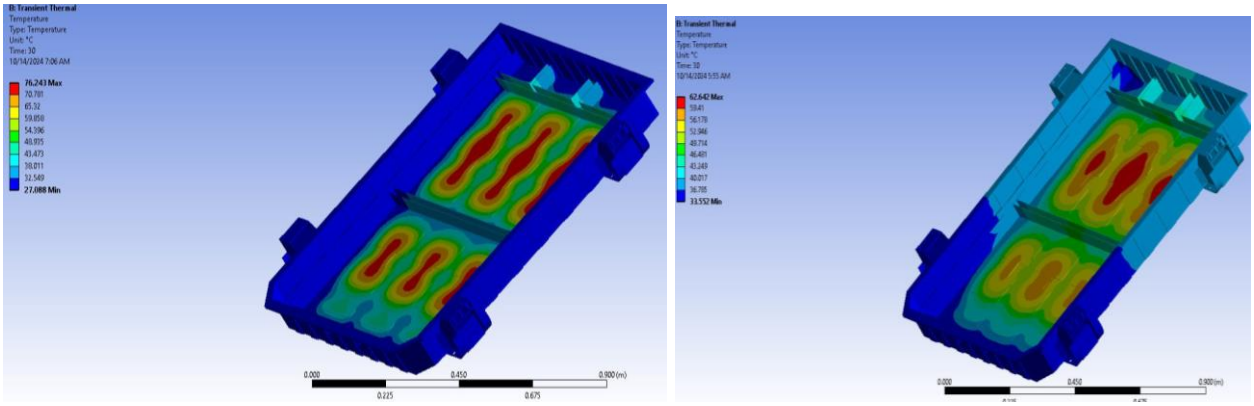

4) Surface temperature of battery tray at 40% SOC discharging under steel4130 and alsic battery tray materials.

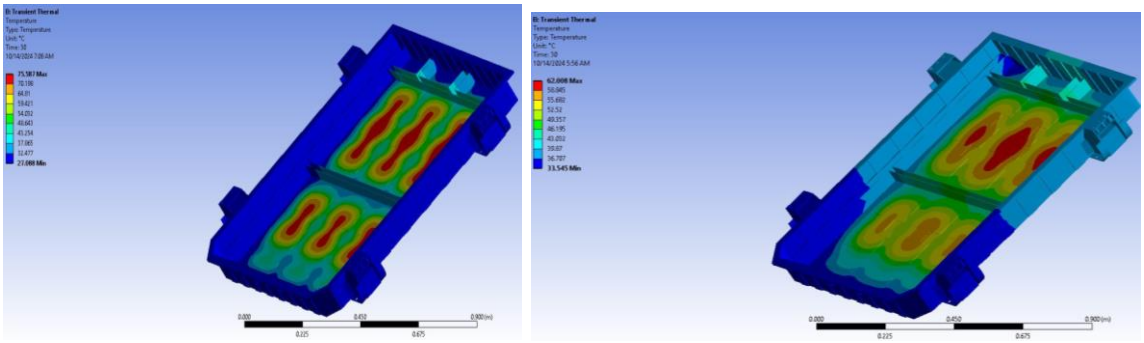

5) Surface temperature of battery tray at 60% SOC discharging under steel4130 and alsic battery tray materials.

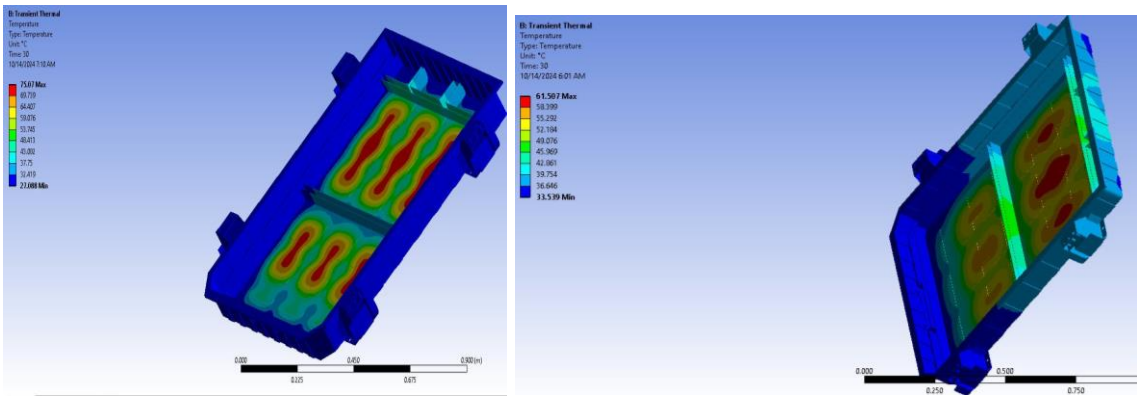

6) Surface temperature of battery tray at 70% SOC discharging under steel4130 and alsic battery tray materials.

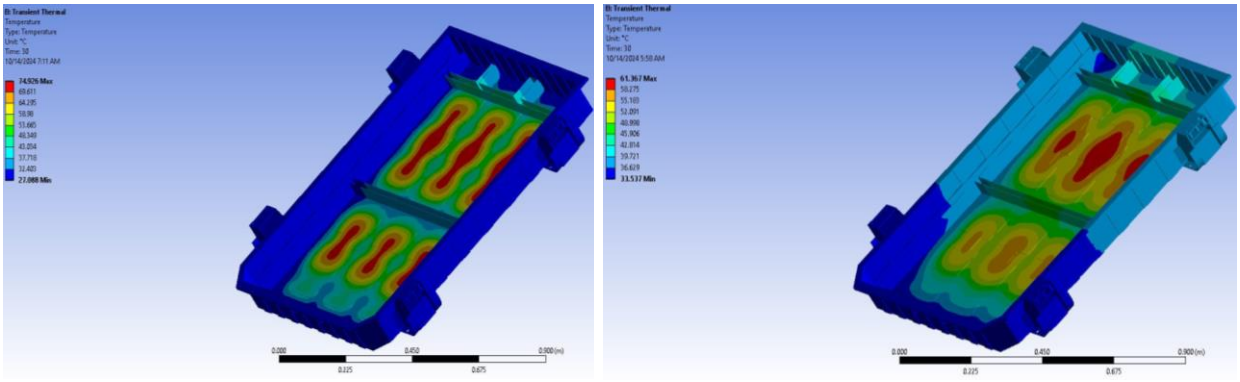

7) Surface temperature of battery tray at 80% SOC discharging under steel4130 and alsic battery tray materials.

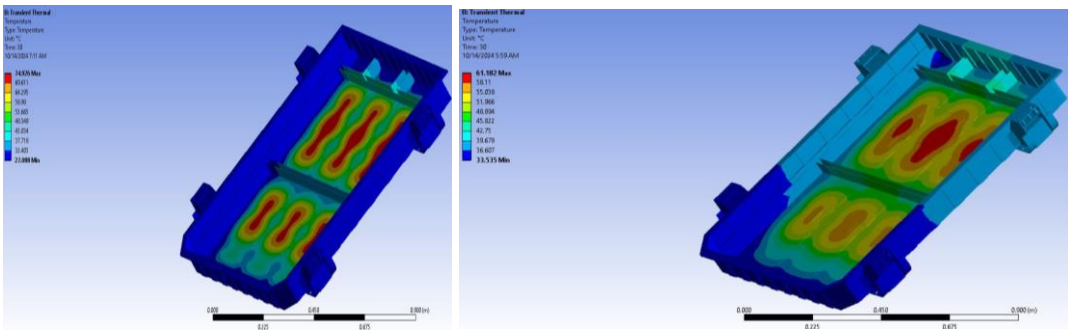

8) Surface temperature of battery tray at 90% SOC discharging under steel4130 and alsic battery tray materials.

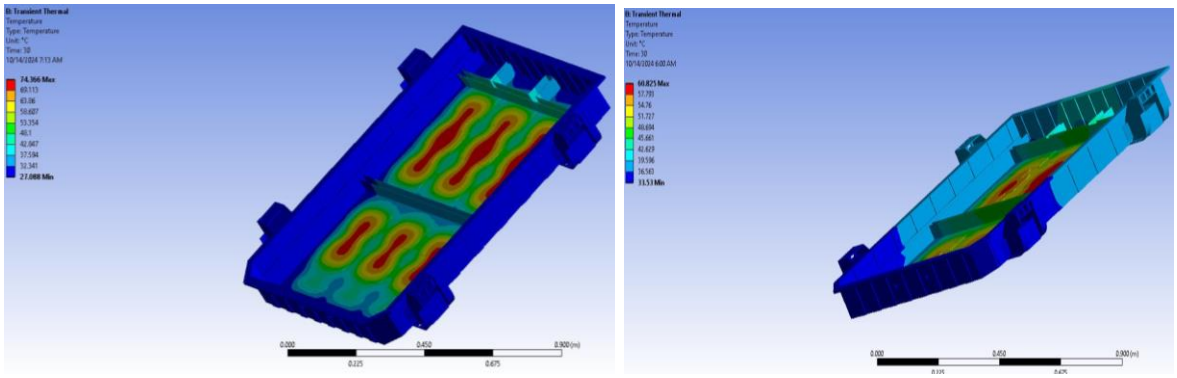

Appendix C

C1; ANSYS fluid flow fluent analysis processes

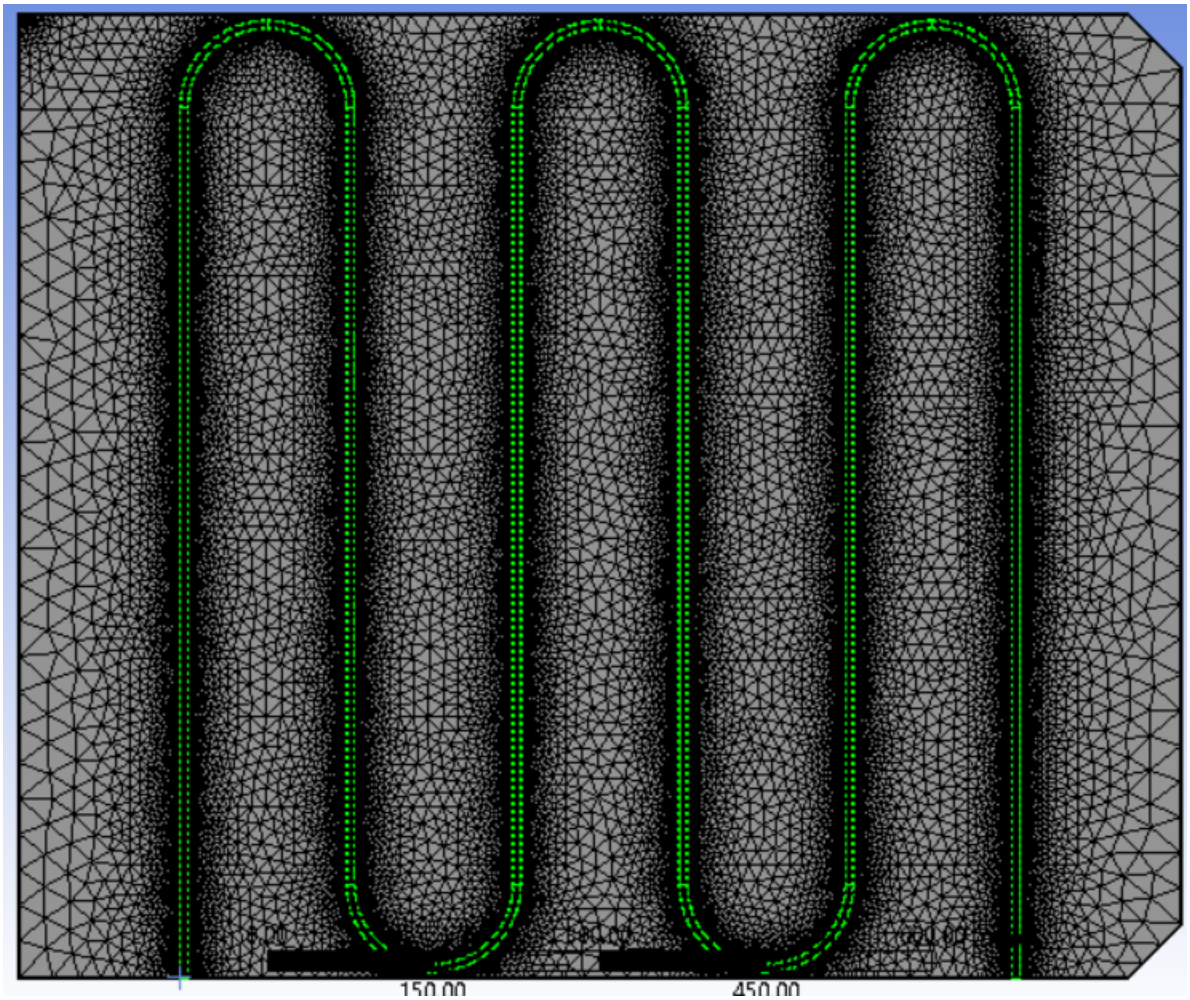

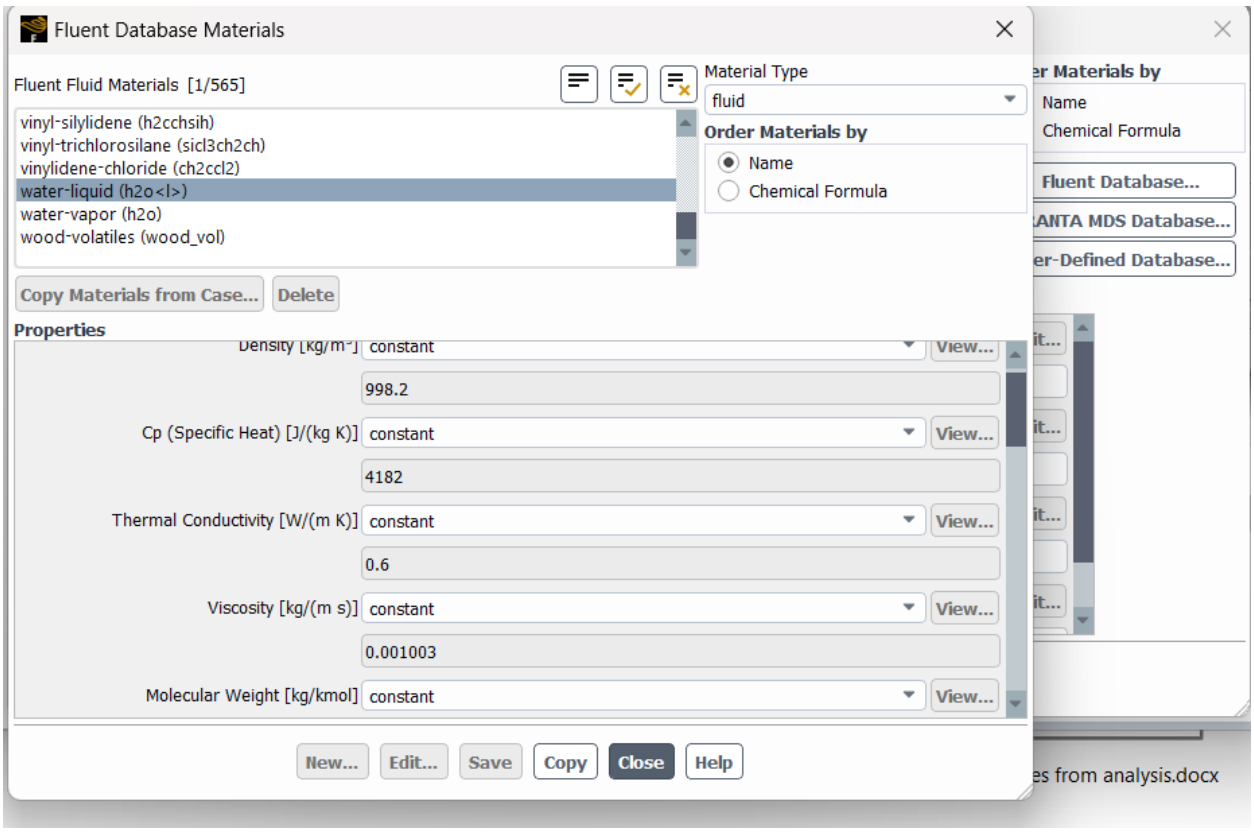
Fluent Database Materials
Fluent Fluid Materials [1/565]
vinyl-silylidene (h2cchsih)
vinyl-trichlorosilane (sicl3ch2ch)
vinylidene-chloride (ch2ccl2)
water-liquid (h2o<l>)
water-vapor (h2o)
wood-volatiles (wood_vol)
Material Type
fluid
Order Materials by
Name
Chemical Formula
Copy Materials from Case...
Delete
Properties
Density [kg/m³] constant
998.2
Cp (Specific Heat) [J/(kg K)] constant
4182
Thermal Conductivity [W/(m K)] constant
0.6
Viscosity [kg/(m s)] constant
0.001003
Molecular Weight [kg/kmol] constant
View...
New...
Edit...
Save
Copy
Close
Help
Fluent Database...
ANTA MDS Database...
er-Defined Database...
es from analysis.docx

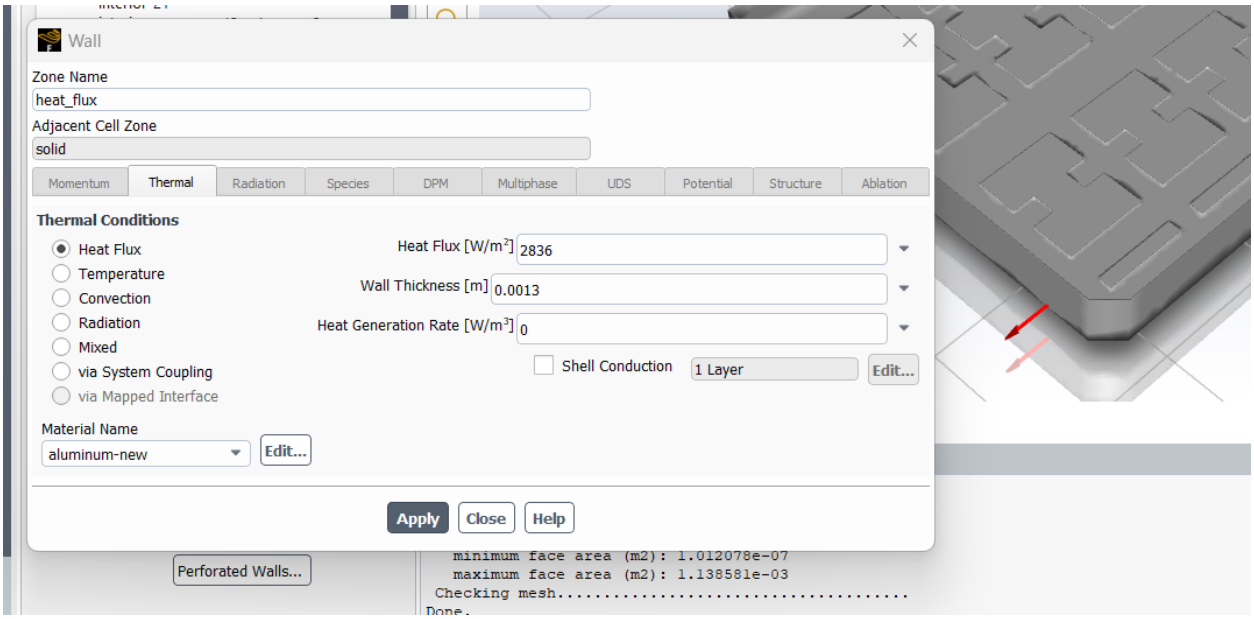
Wall
Zone Name
heat_flux
Adjacent Cell Zone
solid
Momentum
Thermal
Radiation
Species
DPM
Multiphase
UDS
Potential
Structure
Ablation
Thermal Conditions
Heat Flux
Temperature
Convection
Radiation
Mixed
via System Coupling
via Mapped Interface
Heat Flux [W/m²] 2836
Wall Thickness [m] 0.0013
Heat Generation Rate [W/m³] 0
Shell Conduction
1 Layer
Edit...
Material Name
aluminum-new
Edit...
Apply
Close
Help
Perforated Walls...
minimum face area (m2): 1.012078e-07
maximum face area (m2): 1.138581e-03
Checking mesh.....
Done.

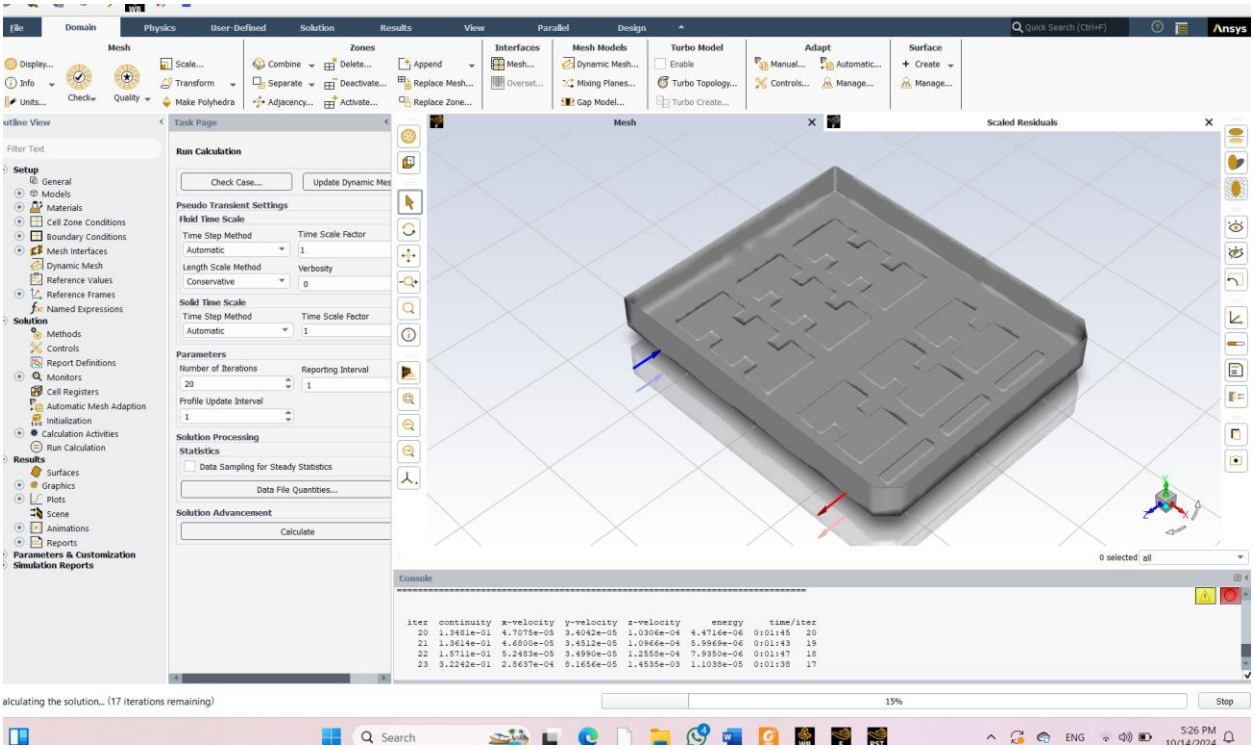
Domain
Physics
User-Defined
Solution
Results
View
Parallel
Design
Mesh
Zones
Interfaces
Mesh Models
Turbo Model
Adapt
Surface
Task Page
Run Calculation
Check Case...
Update Dynamic Mesh...
Pseudo Transient Settings
Fluid Time Scale
Solid Time Scale
Parameters
Number of Iterations
Reporting Interval
Profile Update Interval
Solution Processing
Statistics
Data Sampling for Steady Statistics
Data File Quantities...
Solution Advancement
Calculate
Mesh
Scaled Residuals
Console
iter continuity x-velocity y-velocity z-velocity energy time/iter
20 1.3481e-01 4.7075e-05 3.4042e-05 1.0306e-04 4.4716e-06 0:01:45 20
21 1.3614e-01 4.6800e-05 3.4512e-05 1.0966e-04 5.9969e-06 0:01:43 19
22 1.5711e-01 5.2483e-05 3.4990e-05 1.2558e-04 7.9350e-06 0:01:47 18
23 3.2242e-01 2.8637e-04 8.1656e-05 1.4535e-03 1.1038e-05 0:01:38 17
alculating the solution... (17 iterations remaining)
15%
Stop
Search
ENG
5:26 PM

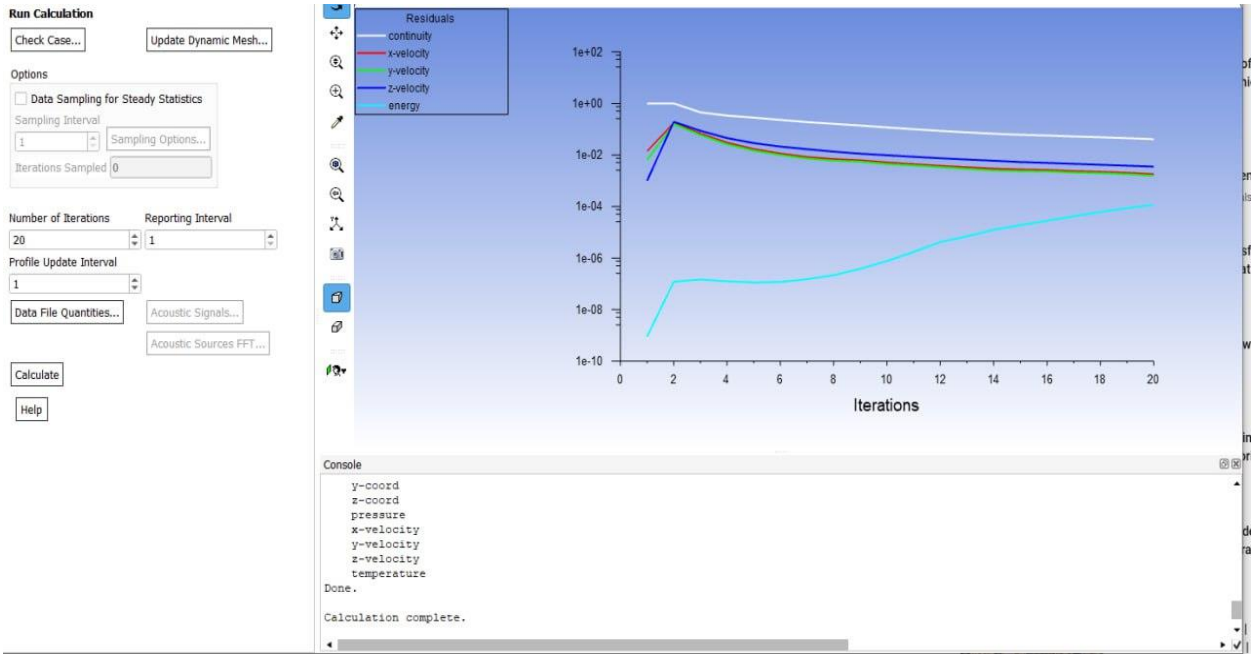
Run Calculation
Check Case...
Update Dynamic Mesh...
Options
Data Sampling for Steady Statistics
Sampling Interval
Sampling Options...
Iterations Sampled
Number of Iterations
Reporting Interval
Profile Update Interval
Data File Quantities...
Acoustic Signals...
Acoustic Sources FFT...
Calculate
Help
Residuals
continuity
x-velocity
y-velocity
z-velocity
energy
1e+02
1e+00
1e-02
1e-04
1e-06
1e-08
1e-10
0
2
4
6
8
10
12
14
16
18
20
Iterations
Console
y-coord
z-coord
pressure
x-velocity
y-velocity
z-velocity
temperature
Done.
Calculation complete.

C2; CFD simulation result

1) Temperature of coolant=10℃

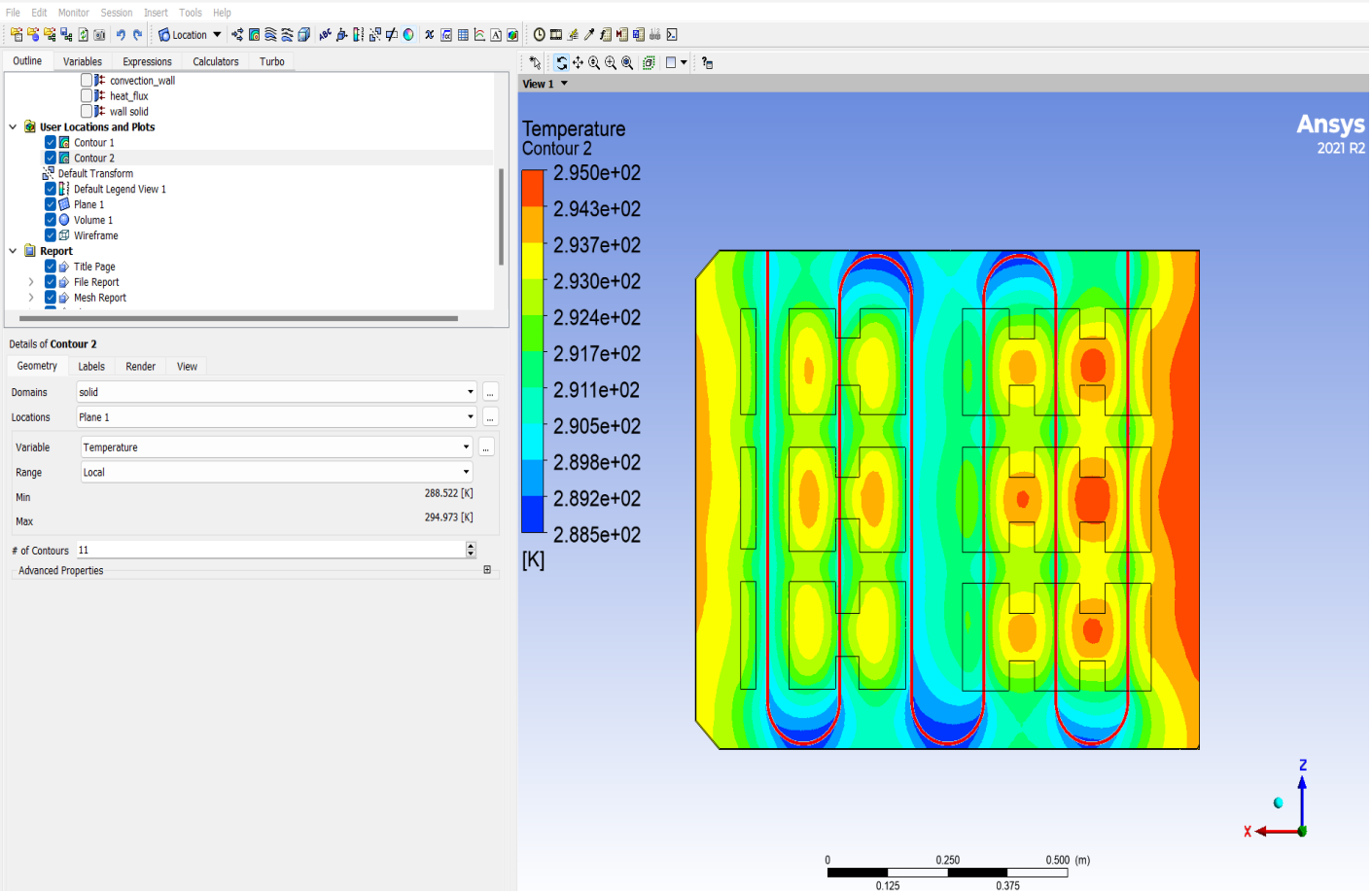

2) Temperature of coolant=15℃

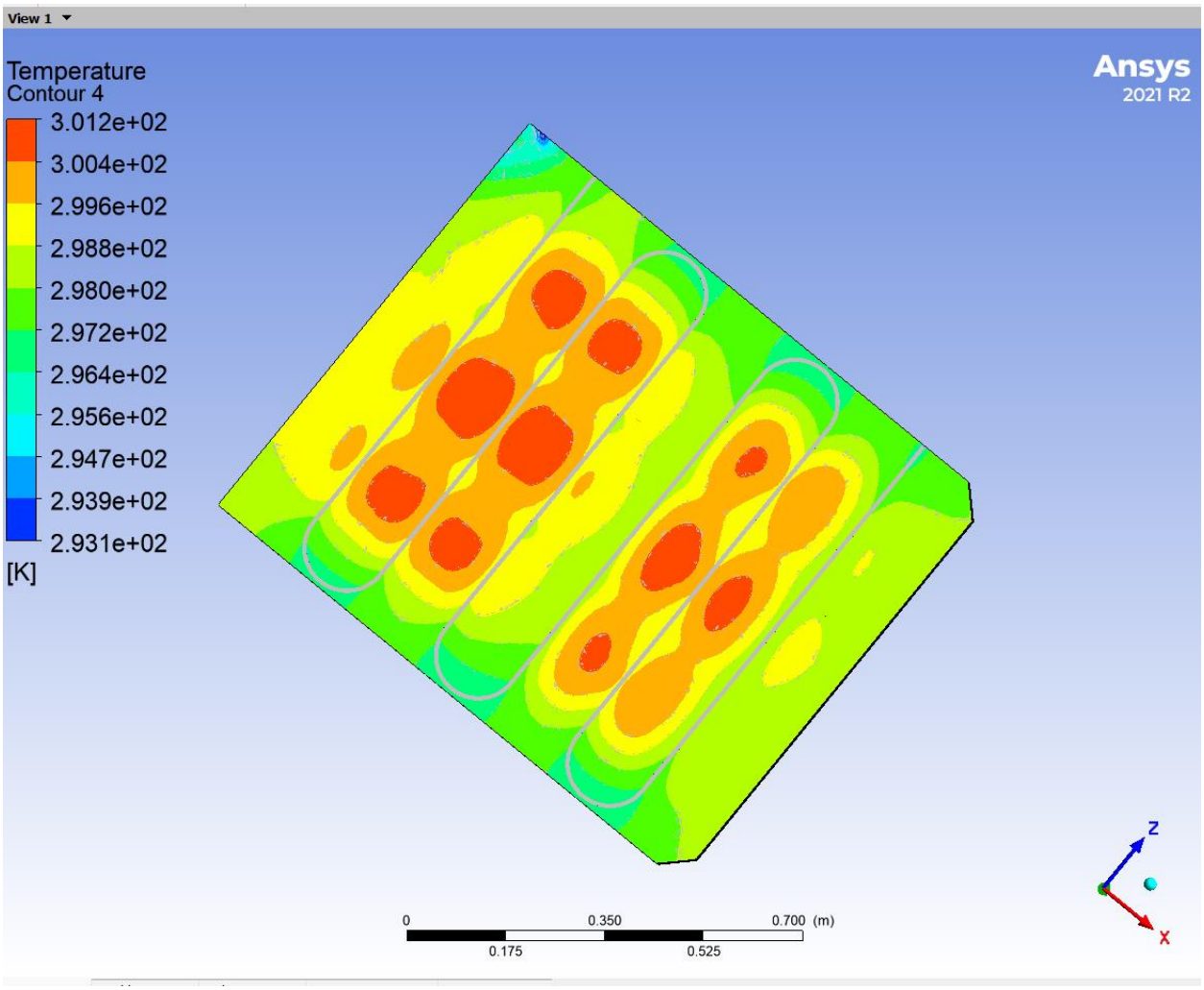

3) Temperature of coolant=20℃